NBS1 Recruits RAD18 via a RAD6-like Domain and Regulates Pol η-Dependent Translesion DNA Synthesis.

AUTHOR(S):

Yanagihara, Hiromi; Kobayashi, Junya; Tateishi, Satoshi; Kato, Akihiro; Matsuura, Shinya; Tauchi, Hiroshi; Yamada, Kouichi; ... Mori, Toshio; Zou, Lee; Komatsu, Kenshi

CITATION:

Yanagihara, Hiromi ...[et al]. NBS1 Recruits RAD18 via a RAD6-like Domain and Regulates Pol η-Dependent Translesion DNA Synthesis.. Molecular cell 2011, 43(5): 788-797

ISSUE DATE:

2011-09-02

URL:

http://hdl.handle.net/2433/145963

NBS1 Recruits RAD18 via a RAD6-Like Domain and Regulates Pol η-dependent Translesion DNA Synthesis

H. Yanagihara[1]*, J. Kobayashi[1]*, S. Tateishi[2], A. Kato[1], S. Matsuura[3], H. Tauchi[4], K. Yamada[5], J. Takezawa[5], K. Sugasawa[6], C. Masutani[7], F. Hanaoka[8], C. M. Weemaes[9], T. Mori[10], L. Zou[11], K. Komatsu[1#]

[1]Radiation Biology Center, Kyoto University, Kyoto 606-8501, Japan

[2]Institute of Molecular Embryology and Genetics, Kumamoto University, Kumamoto 862-0976, Japan.

[3]Research Institute for Radiation Biology and Medicine, Hiroshima University, Hiroshima 734-8553, Japan

[4]Department of Biological Sciences, Ibaraki University, Ibaraki 310-8512, Japan

[5]Division of Genetic Biochemistry, The National Institute of Health and Nutrition, Shinjuku-ku, Tokyo 162-8636, Japan

[6]Biosignal Research Center, Organization of Advanced Science and Technology, Kobe University, Hyogo 657-8501, Japan

[7]Graduate School of Frontier Biosciences and Solution Oriented Research for Science

and Technology, Osaka University, Osaka 565-0871, Japan

[8]Faculty of Science, Gakushuin University, Tokyo 171-8588, Japan.

[9]Department of Pediatric Immunology, Radboud University Nijmegen Medical Centre, 6500 HB Nijmegen, The Netherlands

[10]Radioisotope Research Center, Nara Medical University, Nara 634-8521, Japan.

[11]MGH Cancer Center, Harvard Medical School, MA 02129, USA

[#]To whom correspondence should be addressed

*These authors contributed equally to this work

Address correspondence to: Kenshi Komatsu, Radiation Biology Center, Kyoto University, Yoshida-konoe, Sakyo, Kyoto 606-8501, Japan, Tel. +81-75-753-7550;

RUNNING TITLE: RAD18 recruitment by NBS1.

SUMMARY

Translesion DNA synthesis, a process orchestrated by mono-ubiquitinated PCNA, is critical for DNA damage tolerance. While the ubiquitin-conjugating enzyme RAD6 and ubiquitin ligase RAD18 are known to mono-ubiquitinate PCNA, how they are regulated by DNA damage is not fully understood. We show that NBS1 (mutated in Nijmegen breakage syndrome) binds to RAD18 after UV irradiation and mediates the recruitment of RAD18 to sites of DNA damage. Disruption of NBS1 abolished RAD18-dependent PCNA ubiquitination and Pol η focus formation, leading to elevated UV sensitivity and mutation. Unexpectedly, the RAD18-interacting domain of NBS1, which was mapped to its C-terminus, shares structural and functional similarity with the RAD18-interacting domain of RAD6. These domains of NBS1 and RAD6 allow the two proteins to interact with RAD18 homodimers simultaneously, and are crucial for Pol η -dependent UV tolerance. Thus, in addition to chromosomal break repair, NBS1 plays a key role in translesion DNA synthesis.

INTRODUCTION

The stability of the genome is constantly challenged by both intrinsic and extrinsic stresses. A mammalian cell faces approximately 30,000 spontaneous DNA lesions per day. In addition, many environmental factors, such as ionizing and UV radiation and certain chemicals, can cause DNA damage (Friedberg EC, 2005; Waters et al., 2009). Several cellular processes, including DNA repair, translesion DNA synthesis, and DNA damage signaling, are necessary for cells to cope with DNA damage. Defective damage responses can lead to elevated cell death and genome instability, as observed in a patient with Nijmegen breakage syndrome (NBS), which is characterized by high sensitivity to ionizing radiation (IR) and predisposition to malignancies (Carney et al., 1998; Kobayashi et al., 2004; Matsuura et al., 1998). The cells from a patient with NBS showed defects in DNA repair and checkpoints controls. NBS1, which is mutated in NBS, accumulates at sites of DNA double strand break (DSB) and initiates homologous recombination repair with MRE11, a nuclease involved in DNA resection of DSB ends. The ATM (ataxia telangiectasia mutated) kinase is recruited to sites of DSBs by NBS1,

where it activates the DNA damage checkpoint and regulates DNA repair by phosphorylating specific substrates (Uziel et al., 2003). NBS1 contains a conserved MRE11-binding domain near the C-terminus (682-693 a.a.) and an ATM-binding domain at the extreme C-terminus (734-754 a.a.) (Falck et al., 2005; Richard et al., 2000; Tauchi et al., 2001; Tauchi et al., 2002). Therefore, the roles of NBS1 in homologous recombination and cell-cycle checkpoint regulation are associated with the presence of two binding domains at the C-terminus. It has been reported that NBS1 is implicated in the response to UV-induced DNA damage as cells depleted of NBS1 by siRNA are sensitive to UV (Biard, 2007; Zhong et al., 2005). However, patient-derived NBS cells, which express low levels of a truncated NBS1 mutant lacking FHA and BRCT1 at the N-terminus, shows normal UV sensitivity. These observations raise the question of whether the C-terminal region of NBS1 has an unknown function in UV tolerance.

Translesion DNA synthesis (TLS) is a DNA damage tolerance mechanism conserved from yeast to mammals. Defects in TLS cause high sensitivity to UV, as observed in a patient with mutated Pol η (Xeroderma pigmentosum variant: XPV)

(Masutani et al., 1999a; Masutani et al., 1999b), and in the RAD18 knockout mouse (Tateishi et al., 2003). TLS is initiated by ubiquitination of the sliding clamp protein PCNA. This causes replication DNA polymerase Pol δ /Pol ε to switch with translesion DNA polymerases, such as Pol η , which is able to carry out DNA synthesis across the damaged DNA (Gearhart and Wood, 2001; McCulloch et al., 2004; Stelter and Ulrich, 2003; Yang and Zou, 2009). The ubiquitin-conjugating E2 enzyme RAD6 and its cognate ubiquitin E3 ligase RAD18 are recruited to sites of stalled replication after exposure to DNA damaging agents, such as UV and hydroxyurea, and mediate mono-ubiquitination of PCNA (Inagaki et al., 2009; Ulrich and Jentsch, 2000). A recent study suggested the $CRL4^{Cdt2}$ E3 ligase also contributes to the basal mono-ubiquitination of PCNA in the absence of DNA damage (Terai et al., 2010). It has been reported that RAD18 directly binds to the ssDNA-binding replication protein A, and is recruited to ssDNA generated at sites of stalled replication by UV-induced damage (Davies et al., 2008). However, a RAD18 mutant lacking the RPA-binding region still forms nuclear foci after UV exposure (Nakajima et al., 2006), suggesting the existence of additional mechanisms that contribute to the recruitment of RAD18. Here

we analyze the NBS1-deficient cells and show that NBS1 interacts with RAD18 through a RAD6-like domain near the C-terminus of NBS1 and recruits RAD18 to UV-induced DNA damage. The similarity between the RAD18-binding domain of NBS1 and RAD6 reveals a protein-protein interaction module shared by the proteins involved in TLS.

RESULTS

High UV-sensitivity of NBS1-deficient cells

To examine the role of NBS1 in response to UV-induced DNA damage, we measured the recruitment of NBS1 to sites of UV-induced DNA damage. When cells were irradiated with UV through 5 μm membrane filters, NBS1 was localized to the subnuclear areas of UV damage, which were detected using a cyclobutane pyrimidine dimer (CPD) antibody (Figure 1A). Similar results were obtained in cells irradiated with UVA laser (Figure S1A). BrdU labeling of cells revealed that the UV-induced NBS1 accumulation was confined to cells undergoing significant DNA synthesis (Figure S1B). Moreover, while the N-terminus of NBS1 was essential for IR-induced NBS1 focus formation, it was dispensable for the localization of NBS1 to sites of UV-induced damage (Figure S1C) (Tauchi et al., 2001). These results suggest that NBS1 is recruited to UV-induced damage and DSBs by distinct mechanisms.

We next analyzed UV-induced cell killing of two cell lines derived from NBS patients, 07166VA7 and 0823HSV. 07166VA7 cells expresses a 70 kDa NBS1 species

that lacks the N-terminal FHA and BRCT1 domains, which is similar to another NBS patient with the 657del5 mutation (Tauchi et al., 2001; Varon et al., 2006). 0823HSV cells are homozygous for the C976T mutation in exon 8, which was predicted to cause a premature truncation at the C-terminus (The International Nijmegen Breakage Syndrome Study Group, 2000; Varon et al., 1998). We were unable to detect any NBS1 in 0823HSV cells by Western blotting, presumably because the truncated protein is expressed at a very low level (Figure 1B). Colony forming assay of these cells after UV exposure revealed high UV sensitivity in 0823HSV cells, but not in 07166VA7 cells (Figure 1B), although 07166VA7 cells are sensitive to ionizing radiation (Tauchi et al., 2001). The difference in UV sensitivity of these two NBS1 mutant cell lines may be attributed to the different expression levels of the truncated NBS1 species.

Similar UV sensitivity was observed in NBS1-deficient mouse cells. A31-1 embryonic fibroblasts (MEFs) were derived from 8.5-dpc embryos of NBS1-deficient mouse (Matsuura et al., 2004). A31-1 MEFs express a 55 kDa form of NBS1 lacking the N-terminus (Figure 1B), which was co-immunoprecipitated with MRE11 (Figure S1D). This corresponds to the 55 kDa NBS1 fragments in NBS patients with the

900del25 mutation in exon 8 or 835del4 in exon 7, which translate truncated proteins from Met296 (Tanzanella et al., 2003; Varon et al., 2006). MEF and ES cells from the NBS1-deficient mice generated by another group (ΔB/ΔB NBS1; Willams et al., 2002) express a 80 kDa form of NBS1 lacking the N-terminus, similar to 07166VA7 cells (Figures 1B and S1E). Although p70 of human NBS1 is translated from the middle of exon 6, downstream of the 657del5 mutation, mouse p80 is translated from the beginning of exon 6 (Williams et al., 2002). These MEFs from NBS1-defcient mouse express different truncated NBS1 at low levels, and the level of ΔB/ΔB NBS1 is higher in ES cells than in MEFs (Figure S1E). Both A31-1 and ΔB/ΔB MEF cells showed elevated sensitivity to UV and their hypersensitivities were suppressed by the introduction of full-length human NBS1 cDNA (Figures 1B, 1C, and S1F). This UV sensitivity of NBS1-deficient MEFs is unlikely due to the presence of truncated NBS1 fragments but rather to the decreased of NBS1 levels, since knockdown of NBS1 in HeLa cells using siRNA resulted in high UV sensitivity (Figures 1D and S2A), which is consistent with previous reports (Biard, 2007; Zhong et al., 2005). Furthermore, the UV sensitivity of HeLa cells treated with NBS1 siRNA correlates with the extents of NBS1

knockdown and it was restored by siRNA-resistant NBS1 (Figures 1D, S2B and S2C). Since the cell-cycle distributions of NBS1-deficient cells and HeLa cells with reduced NBS1 were not significantly altered compared to control cells, the defects in UV response were not due to the altered cell-cycle (Figures S2D and S2E). Thus, NBS1-deficient human and mouse cells with low levels of NBS1 are hypersensitive to UV, suggesting a critical role of NBS1 in the response to UV-induced damage.

Deficiency of NBS1 abolished RAD18-dependent PCNA ubiquitination and Pol η focus formation

UV-induced DNA damage is predominantly removed by nucleotide excision repair (NER) and thus, the UV sensitivity of NBS1-deficient cells might be indicative of defective NER. We determined the NER activities of NBS1-deficient cells by ELISA using antibodies to (6-4)-photoproduct (6-4PP). The removal of 6-4PP was similar in OCN1 cells (mouse NBS1$^{+/-}$), A31-1 cells, and the A31-1 cells complemented with the NBS1 p70 fragment, which corresponds to the 70 kDa NBS1 species in NBS patients (Figures S3A and S3B). In contrast, the removal of 6-4PP was significantly decreased in

XPC$^{-/-}$ knockout MEFs (Figure S3A). These results indicated intact NER activity in A31-1 cells. Subsequently, we analyzed TLS in OCN1, A31-1 and complemented A31-1 cells using UV-induced Pol η foci as a marker (Nishi et al., 2009). Focus formation of Pol η was robustly induced in OCN1 cells after exposure to UV, but was impaired in A31-1 cells (Figures 2A and S3C). This defect of Pol η focus formation in A31-1 cells was rescued by NBS1 cDNAs (both full length and p70). Consistently, A31-1 cells showed severely reduced mono-ubiquitination of PCNA. The defect of mono-ubiquitination of PCNA was also completely corrected by full length NBS1 cDNA (Figure 2B). The same restoration was also observed by expression of NBS1 p70, indicating that the function of NBS1 in TLS is retained in this fragment. Because PCNA is mono-ubiquitinated by RAD18, we next examined the formation of RAD18 foci in A31-1 cells. UV-induced RAD18 foci were abolished in A31-1 cells after exposure to UV, and this defect in RAD18 focus formation was corrected by NBS1 cDNAs (full length and p70) (Figures 2C and S3D). In HeLa cells treated with NBS1 siRNA, RAD18 also failed to form foci after exposure to 20 J/m^2 UV (Figures 2D and right panel of S3D). RAD18 foci were also observed in HeLa cells irradiated with 5 J/m^2

(Figure S3E). In response to treatment with hydroxyurea (HU), A31-1 cells were also defective in PCNA ubiquitination and RAD18 focus formation, and were highly sensitive to HU (Figures S3F-S3H). Thus, NBS1 is required for RAD18-dependent PCNA mono-ubiquitination and Pol η focus formation.

Deficiencies of NBS1 and Pol η result in similar defects in UV response

As PCNA-mediated Pol η focus formation was compromised in NBS1-deficient cells, we next performed epistatic analysis of cells treated with NBS1 siRNA and/or Pol η siRNA. Knock down of NBS1 or Pol η elevated UV sensitivity to similar extents (Figure 3A). Simultaneous knock down of NBS1 and Pol η did not further increase UV sensitivity (Figure 3A). These results suggest that NBS1 and Pol η function in the same pathway in UV response. Similar results were obtained when UV-induced mutation was analyzed using the *rpsL* gene-containing HITEC mouse cells. Depletion of NBS1 and Pol η elevated mutation frequency to similar extents after UV irradiation and resulted in similar mutation spectrums in the *rpsL* gene (Figure 3B). These phenotypes of NBS1- and Pol η –depleted cells resemble those of XPV cells, which lack

functional Pol η (Friedberg EC, 2005; Wang et al., 2007). Furthermore, when NBS1 and Pol η were concurrently knock-downed, the mutation frequency remained the same as in cells depleted of NBS1 or Pol η alone, suggesting both proteins function in the same pathway (Figure 3B). To confirm the role of NBS1 in TLS, we next performed the experiment with alkaline sucrose velocity sedimentation at 5 hrs after exposure to 5 J/m^2 (Figure S4). This analysis revealed a significant decrease in translesion DNA synthesis in NBS1-deficient A31-1 cells. The medium length of pulse labeled DNA fragments reduced from 1.0 Mb in control cells to 0.36 Mb in NBS1-deficient cells. Thus, NBS1 functions in the Pol η -dependent TLS pathway during UV response.

NBS1 interacts with RAD18 through the conserved region near the C-terminus of NBS1

Since NBS1 is required for the formation of UV-induced RAD18 foci, the physical interaction between NBS1 and RAD18 was examined by co-immunoprecipitation using an RAD18 antibody. NBS1 co-precipitated with RAD18 2 hrs after UV irradiation and the interaction decreased thereafter (Figures 4A). This interaction was not mediated

by DNA and was more readily detected in the chromatin fractions than in the soluble fractions of UV-irradiated cells (Figure S5A). When Myc-tagged RAD18 was expressed in 293E cells, it interacted with Flag-tagged p70 of NBS1 (Figure S5B). Moreover, the UV hypersensitivity of A31-1 cells was suppressed by p70 and the even shorter p55 (Figure S5C). To map the RAD18-interacting region in NBS1, we next generated several C-terminal deletion mutants of NBS1 (Figures 4B, 4C, and S5D). Co-immunoprecipitation experiments using these deletion mutants revealed that the amino acids 650 to 665 a.a. of NBS1 (D2-2 mutant) are important for the interaction of NBS1 with RAD18 (Figure 4C). Moreover, RAD18 failed to localize to sites of UV-induced damage in A31-1 cells and in A31-1 cells expressing the NBS1 mutants lacking the RAD18-binding region (D2 and D2-2 mutants) (Figure 4D). While unable to bind and localize RAD18, the D2 mutant retains the ability to bind MRE11 and RPA, and to activate ATM (Figures 4C and S5E-G). Mirin, an inhibitor of the MRE11 nuclease, did not block PCNA mono-ubiquitination (Figure S5H). Consistent with this observation, when NBS1 (Flag) and RAD18 (Myc) were co-expressed in MRE11-deficient ATLD cells, NBS1 was co-immunoprecipitated with RAD18, as was

that in MRE11-proficient HeLa cells (Figure S5I). Moreover, ATLD cells were sensitive to IR but not UV, although UV-sensitivity was considerably enhanced when NBS1 was depleted with siRNA (Figure S5J). Thus MRE11-deficient phenotypes are similar to that of NBS1 D3 mutant lacking MRE11-binding domain, which was able to bind to RAD18 and showed normal UV-sensitivity (Figures 4C and 4E). Together, these evidences suggest that NBS1 functions in TLS through the RAD18-binding region, which is not directly associated with the functions of MRE11 and ATM.

Blast analysis of the RAD18-binding region of NBS1 (639-665 a.a.) revealed that it is conserved from amphibians to mammals, but not in yeast and flies (Figure 5). Both NBS1 D2-2 mutant and p55 lacking this RAD18-binding region failed to suppress the UV hypersensitivity of A31-1 cells (Figures 4E and S5C). Deletion of amino acids 639 to 649 (the D2-1 mutant), the less conserved half of the RAD18-binding region, slightly reduced the binding of NBS1 to RAD18 (Figures 4C and 5). Nonetheless, the NBS1 D2-1 mutant was able to restore RAD18 focus formation in A31-1 cells, and to suppress the UV hypersensitivity of these cells (Figures 4D and 4E). In contrast, the NBS1 D2-2 mutant lacking the more conserved half of the RAD18-interacting region (a.

a. 650-665) failed to support PCNA mono-ubiquitination and Pol η focus formation (Figures S6A and S6B). The NBS1 D2-2 mutant is efficiently localized to sites of UV-induced DNA damage (Figure S6C), indicating that the localization of NBS1 does not require RAD18 binding. These results suggest that RAD18 is recruited to sites of UV-induced damage by NBS1 via the region encompassing a. a. 650-665.

NBS1 interacts with RAD18 via a RAD6-like domain

To map the NBS1-binding region of RAD18, we generated a set of Myc-tagged RAD18 mutants lacking various known functional domains (Figure 6A). Surprisingly, only the RAD18 mutant lacking the RAD6-binding domain failed to co-immunoprecipitate NBS1 (Figure 6B). We noticed that the RAD18-binding region of NBS1 exhibits significant sequence homology with RAD6 (59-83 a.a.) (Figure 5). Secondary structure modeling of the RAD18-binding region of NBS1 using the SSpro8 program (Baldi et al., 1999) predicts two α-helices with a short linker sequence (Figure 5), which is also similar to two helical structures adjacent to the active site of Cys-88 in RAD6 (Worthylake et al., 1998). To assess the functions of these conserved

domains in NBS1 and RAD6, we generated peptides from the RAD18-binding domains of NBS1 and RAD6, and tested their effects on the interaction of RAD18 with the C-terminus of NBS1, in which NBS1 directly bound to RAD18 in vitro and in cells (Figures 6C and S6D). As expected, the interaction between NBS1 and RAD18 was weakened by the peptide derived from NBS1 (10 μg/ml; N1:PKKLLLTEFRSLV) (Figure 6D). Furthermore, the RAD6-derived peptide (10 μg/ml; R1:DVSSILTSIQSLL) strongly interfered with the interaction between NBS1 and RAD18. The control peptide (C:AKEESLADDLFRY), which contains the ATM-binding sequence of NBS1, did not affect the interaction between RAD18 and NBS1. Therefore, RAD18 interacts with RAD6 and NBS1 through the conserved domains in these proteins, and RAD6 and NBS1 may compete for the same binding surface of RAD18.

Simultaneous interaction of RAD6 and NBS1 with RAD18 homodimers

It is puzzling how RAD18 can be recruited by NBS1 and function with RAD6 if binding to NBS1 and RAD6 are mutually exclusive. To test if a single RAD6-binding domain of RAD18 is used for interaction with both NBS1 and RAD6, the association of

Flag-tagged NBS1 with T7-tagged RAD6 was examined by co-immunoprecipitation in 293E cells (Figure 7A). Surprisingly, NBS1 interacted with RAD6 after UV exposure, and the interaction required RAD18. Importantly, the interaction between NBS1 and RAD6 requires not only the RAD6-binding domain of RAD18, but also its zinc finger domain (Figure 7A). Given that RAD18 forms homodimers through the zinc finger domain (Miyase et al., 2005; Ulrich and Jentsch, 2000), our results suggest that RAD18 homodimers might simultaneously interact with both NBS1 and RAD6. To test this possibility, Myc-tagged RAD18 and Flag-tagged RAD18 were co-expressed in 293E cells. Myc-RAD18 was co-precipitated with Flag-RAD18 when full-length RAD18 was expressed, confirming the formation of RAD18 homodimers in UV-irradiated cells (Figure 7B). When RAD18 dimerization was abolished by deletion of the zinc finger domain (Figure 7B), the interaction between RAD6 and NBS1 was lost (Figure 7A). Accumulation of RAD18 in chromatin is also dependent upon the RAD6/NBS1-binding domain of RAD18 (Figure 7B). The focus formation of the RAD18 mutant lacking the zinc finger domain was severely delayed compared to wild-type RAD18 (Figure 7C). Together, these results suggest that RAD18 dimerization is important for formation of

the NBS1-RAD18-RAD18-RAD6 complex and the accumulation of this complex at sites of UV-induced DNA damage (Figure S7).

DISCUSSION

NBS1 expression and Pol η -dependent TLS

The relevance of NBS1 in UV response is supported by the similar cellular and clinical phenotypes of patients with defective Pol η and NBS1. Patients with XPV (defective Pol η) are characterized by high sensitivity to UV, and patients with NBS also display a weak sun-sensitive skin reaction, as firstly described by C. Weemaes (Weemaes et al., 1981). We found that 0823HSV cells expressing undetectable amounts of NBS1 are highly sensitive to UV, whereas GM07166 cells with significant levels of truncated NBS1 p70 are not. These results suggest that while the N-terminus of NBS1 is dispensable for UV response, the overall level of NBS1 is important. Consistent with this idea, MEFs from two independently generated NBS1-deficient mice with low levels of truncated NBS1 and human cells treated with NBS1 siRNA are all hypersensitive to UV (Figures 1B-1D and S1F). Although it was reported that ΔB/ΔB NBS1 ES cells

are not hypersensitive to UV (Brugmans, et al., 2009), we found that ΔB/ΔB NBS1 MEFs are highly UV-sensitive. This difference could be attributed to the different expression levels of the ΔB/ΔB NBS1 protein in MEFs and ES cells (Figure S1E).

Our results suggest that NBS1 and Pol η function in the same pathway during UV response. Hypermutability is a hallmark of XPV cells; the UV-induced mutation frequency in XPV cells is considerably higher than that in wild-type cells (Wang et al., 2007). In our mutation experiment using *rpsL* gene-containing mouse cells, NBS1-deficient cells showed high frequency of mutation, and the mutagenic spectrum was similar to that of Pol η -deficient cells. Moreover, double knockdown of NBS1 and Pol η revealed that these two proteins function in a common pathway in response to UV lesions. It has been reported that RAD18 and Pol η have roles in both homologous recombination and TLS (McIlwraith et al., 2005; Szuts et al., 2006). Since we previously reported a pivotal role of NBS1 in homologous recombination, the UV hypersensitivity of NBS1-defective cells might be due to defective homologous recombination. However, the binding of NBS1 to MRE11, a protein implicated in the initiation of homologous recombination, is intact in the NBS1 mutant unable to bind

RAD18 and hypersensitive to UV. Furthermore, both NBS1 mutant lacking the MRE11-binding domain and MRE11-deficient ATLD cells were not sensitive to UV, although ATLD cells were sensitive to IR (Figures 4E and S5J). Importantly, sucrose gradient sedimentation analysis provided direct evidence that translesion DNA synthesis is defective in NBS1-defective cells. Together, these results suggest that NBS1 has a direct role in Pol η -dependent TLS.

A role of NBS1 in RAD18 recruitment

Our *in vivo* and *in vitro* experiments suggest that NBS1 and RAD6 interact with the same surface of RAD18 (Figures 5, 6B-6D and S6D). Disruption of the NBS1-RAD18 interaction led to defective PCNA ubiquitination, compromised focus formation of RAD18 and Pol η , and enhanced cell killing by UV (Figures 2, S3C and S3D). We speculate that RAD18 may simultaneously associate with NBS1 and RAD6 to carry out its function in PCNA ubiquitination (Figure S7). Consistent with this hypothesis, we find that RAD18 homodimers formed through the zinc finger domains can interact with NBS1 and RAD6 simultaneously. It is important to note that the

RAD18 mutant lacking the zinc finger domain is able to support PCNA ubiquitination in cells. While the RAD18 mutant lacking the zinc finger failed to form foci shortly after exposure to UVA or UVC (Miyase et al., 2005; Nakajima et al., 2006), it was localized to site of UV-induced damage at later time points (Figure 7C). These results suggest that RAD18 dimerization is not strictly required for its function in PCNA ubiquitination, and that the zinc finger-independent focus formation of RAD18 may contribute to PCNA ubiquitination. The delay of RAD18 focus formation in the absence of the zinc finger suggests that RAD18 dimerization and/or the RAD18-RAD6 interaction facilitates RAD18 accumulation on damage DNA. In the absence of the zinc finger, RAD18 monomers may be recruited by NBS1 and subsequently dissociate from NBS1 to form a functional complex with RAD6.

NBS1 likely functions upstream of RAD18 because NBS1 is required for RAD18 focus formation, whereas RAD18 is not needed for NBS1 recruitment to UV lesions (Figures 2 and S6C). How NBS1 is recruited to sites of UV damage remains unclear. The FHA/BRCT domains of NBS1 are important for NBS1 recruitment/retention to DSBs, but not to UV lesions (Figures S1C and S7) (Tauchi et

al., 2001). It has been reported that RPA1 can directly interact with NBS1 (Oakley et al., 2009), suggesting that NBS1 might be recruited to the RPA-coated single-stranded DNA at sites of UV induced damage (Figure S7). The previously reported interaction between RAD18 and RPA may function together with NBS1 to recruit RAD18-RAD6, or play an important role in stabilizing the RAD18-RAD6 complex on damaged DNA (Davies et al., 2008).

The conserved domains of NBS1

The RAD6-like domain of NBS1 is only found in vertebrate NBS1, whereas the MRE11-binding domain at the C-terminus and FHA/BRCT domains at the N-terminus are conserved from yeast to humans (Tauchi et al., 2002). This RAD6-like domain of NBS1 may have emerged in vertebrate NBS1 to orchestrate TLS with other NBS1 functions in regulation of ATM-mediated checkpoint/apoptosis and MRE11-mediated homologous recombination repair. Interestingly, the RAD18-binding domain of NBS1 is always retained in the truncated NBS1 species in the viable NBS1-deficient cells. Recently, we identified an RNF20-binding domain at the C-terminus of NBS1, which

regulates the chromatin reorganization during homologous recombination repair (Figure 4B) (Nakamura et al., 2011). Further analysis of the C-terminus of NBS1 may shed lights on the coordination among TLS, DNA repair, checkpoint signaling, and chromatin remodeling.

EXPERIMENTAL PROCEDURES

Cell Culture and Transfection

A31-1 cells (NBS1-deficient cells derived from $NBS1^{-/-}$ mouse), OCN1 cells ($NBS1^{+/-}$), $BN^{+/+}$ cells ($NBS1^{+/+}$) and $RAD18^{-/-}$ cells were established from lung fibroblasts of NBS1-deficient (chimera) mouse (Matsuura et al., 2004) and Rad18 knockout mouse (Tateishi et al., 2003), respectively. The NBS cell lines, 07166VA7, were established from the fibroblasts of patients with NBS (Tauchi et al., 2002). Similarly, 0823HSV was established from skin fibroblast of Dutch patient with NBS1 (Weemaes et al., 1994). The NBS1-deficient MEF cells and ES cells, ΔB/ΔB, were generously provided by Dr. J. Petrini and Dr. Dik van Gent (Brugmans et al.,

2009; Williams et al., 2002). The *rpsL* gene-containing MEF cells were established from lung fibroblast of HITEC mouse (Gondo et al., 1996). ATLD2 cells were kindly provided by Dr. P. Concannon. Human HeLa cells and 293E cells were used as control cell lines. All cell lines were cultured in Dulbecco's modified Eagle's medium (Sigma Chemical Co.) supplemented with 10% fetal bovine serum (HyClone) at 37°C in a humidified atmosphere containing 5% CO_2. The cDNAs of NBS1, RAD18 and RAD6 were transfected into A31-1 cells and 293E cells using Lipofectamine 2000 (Invitrogen).

Antibodies and immunoprecipitation assay

The human/mouse anti-RAD18, anti-CPD and anti-Pol η antibodies were described previously (Mori et al., 1991; Ohkumo et al., 2006; Tateishi et al., 2003; Tateishi et al., 2000). Other antibodies and reagents were purchased from the following manufacturers: anti-NBS1 (Novus Biologicals: NB100-143, Gene Tex:GTX7022, R&D Systems:MAB1573), anti-MRE11 (Novus Biologicals: NB100-142, Gene Tex: 12D7), anti-PCNA PC-10 (Santa Cruz Biotechnology:sc-56), anti-β-actin (Sigma:A5316),

anti-T7 (Novagen:69522-3), anti-c-Myc 9E10 (Covance:MMS-150R), polyclonal anti-Flag (Sigma:F7425) and monoclonal anti-Flag M2 (Sigma:F1804). For the immunoprecipitation assay, 293E cells were transfected with 8 μg of plasmid using Lipofectamine 2000, and 48 hrs later cells were washed with cold PBS and lysed on ice for 30 min in IP-buffer (20 mM Hepes-NaOH(pH7.4), 0.2% NP-40, 150 mM NaCl, 25% glycerol, 1 mM EDTA, 1x protease inhibitor, 10 mM NaF, 1 mM Na_3VO_4). Soluble material was recovered by centrifugation at 3000 G for 5 min. The pellet was washed twice with lysis buffer and extracted with IP-buffer for 30 min on ice. After sonication and subsequent centrifugation, this chromatin fraction was diluted with IP-buffer and proteins were immunoprecipitated for 2 hrs with RAD18 antibody, T7 antibody or c-Myc antibody.

Immunostaining

Cells on cover slips were washed with PBS, fixed in 4% formalin and incubated with a detergent solution at 4°C for 5 min. After treatment with a blocking solution for 30 min, cells were exposed to the appropriate primary antibody against NBS1 or RAD18 and the

fluorescent secondary antibody, Alexa-488-conjugated anti-rabbit IgG (Invitrogen). For detection of replicating cells, cells were labeled and immunostained according to the method described by the 5-bromo-2′ deoxy-uridine labeling and detection kit I (Roche Diagnostics: Mannheim, Germany). eGFP-Pol η expression plasmid was kindly provided by Dr. C. Masutani (Osaka University). For visualization of GFP-fusion proteins, OCN1 cells and A31-1 cells transiently expressing eGFP-Pol η grown on a coverslip were rinsed twice with PBS and fixed by soaking with 4% formaldehyde at 4°C for 20 min. After washing, the cells were mounted on a slide glass. Fluorescence was visualized with a confocal laser-scanning microscope (Olympus: Fv300). At least 200 cells were counted for quantification of focus positive cells, which are defined as more than 10 foci-containing cells.

RNAi knockdown of NBS1

A mixture of siTrio RNA oligonucleotides (B-Bridge international) were transfected into cells using Lipofectamine 2000 or Lipofectamine RNAi MAX (Invitrogen).

The following siRNA sequences were used: Human NBS1 siRNA mixture (#1:5′ -

GUACGUUGUUGGAAGGAAA, #2: 5′ - GGGAAAGGGAUGAAGAAAA, #3: 5′ -GGACACAAAACCAGAGUUA), mouse NBS1 siRNA mixture (#1:5′ -CGUUGUUGAUGUAGGAAUUA, #2: 5′ -GGGAAAGGGAUGAAGACAA, #3: 5′ -GAUCAGAGCCGGAAAGCAA), mouse Pol η siRNA mixture (#1:5′ -GAAUAAACCUUGUGCAGUU, #2: 5′ -GAAAGAGGCUAUUCGGAAA, #3: 5′ -GGAUAGAAUACAUGGGUGA) and non-targeting siRNAs as a control.

The siRNA-resistant NBS1 expression plasmid was generated by introducing neutral mutations in the siRNA-targeting regions.

Mutation Frequency Assays

HITEC MEFcells were transfected with siRNAs as described above. 24 hrs later, cells were irradiated with UV (5 J/m^2). 72 hrs after, cells were harvested. Analysis of mutation was performed as described previously (Gondo et al., 1996; Murai et al., 2000). For analysis of mutation spectrum, the *rpsL* coding region and its surrounding sequence (from position −120 to position 375) in each mutant plasmid were determined using an automated DNA sequencer (3100-Avant Genetic Analyzer AB).

Peptide inhibitory experiments

Recombinant RAD18 (0.1 mg) protein were mixed with the indicated amount of peptides (N1: PKKLLLTEFRSLV [predicted RAD18-binding site in NBS1], R1: DVSSILTSIQSLL [RAD18-binding site in RAD6], C: AKEESLADDLFRY [ATM-biding site]) and then left on ice for 1 hr. After that, 0.5 mg recombinant GST-tagged C-terminal NBS1 (354-754 a.a.) was added to these mixtures and the RAD18/NBS1 complex were precipitated using Glutathione-Sepharose (GE Healthcare: 17-5132-01). RAD18 present in these precipitates was detected by Western blot analysis using an anti-RAD18 mouse monoclonal antibody (Abnova Co: H00056852-M01).

SUPPLEMENTARY DATA

Supplementary figures can be found with this article on line.

ACKNOWLEDGMENTS

The authors wish to thank Dr. John Petrini, Dr. Dik C. van Gent, and Dr. Kanji Ishizaki for providing ΔB/ΔB MEF, ΔB/ΔB ES cell and retrovirus vector pCLXSL-hTERT. We also thank Yukiko Hayuka and Douglas V.N.P. Oliveira for the excellent technical assistance and discussions. This work was supported by grants from the Ministry of Education, Culture, Sports, Science, and Technology of Japan.

REFERANCES

Baldi, P., Brunak, S., Frasconi, P., Soda, G., and Pollastri, G. (1999). Exploiting the past and the future in protein secondary structure prediction. Bioinformatics *15*, 937-946.

Biard, D.S. (2007). Untangling the relationships between DNA repair pathways by silencing more than 20 DNA repair genes in human stable clones. Nucleic Acids Res *35*, 3535-3550.

Brugmans, L., Verkaik, N.S., Kunen, M., van Drunen, E., Williams, B.R., Petrini, J.H., Kanaar, R., Essers, J., and van Gent, D.C. (2009). NBS1 cooperates with homologous recombination to counteract chromosome breakage during replication. DNA Repair (Amst) *8*, 1363-1370.

Carney, J.P., Maser, R.S., Olivares, H., Davis, E.M., Le Beau, M., Yates, J.R., 3rd, Hays, L., Morgan, W.F., and Petrini, J.H. (1998). The hMre11/hRad50 protein complex and Nijmegen breakage syndrome: linkage of double-strand break repair to the cellular DNA damage response. Cell *93*, 477-486.

Davies, A.A., Huttner, D., Daigaku, Y., Chen, S., and Ulrich, H.D. (2008). Activation of ubiquitin-dependent DNA damage bypass is mediated by replication protein a. Mol Cell *29*, 625-636.

Falck, J., Coates, J., and Jackson, S.P. (2005). Conserved modes of recruitment of ATM, ATR and DNA-PKcs to sites of DNA damage. Nature *434*, 605-611.

Friedberg EC, W.G., Siede W, Wood RD, Schultz RA, Ellenberger T (2005). DNA Repair and Mutagenesis. Washington, DC: ASM Press.

Gearhart, P.J., and Wood, R.D. (2001). Emerging links between hypermutation of antibody genes and DNA polymerases. Nat Rev Immunol *1*, 187-192.

Gondo, Y., Shioyama, Y., Nakao, K., and Katsuki, M. (1996). A novel positive detection system of in vivo mutations in rpsL (strA) transgenic mice. Mutat Res *360*, 1-14.

Inagaki, A., van Cappellen, W.A., van der Laan, R., Houtsmuller, A.B., Hoeijmakers, J.H., Grootegoed, J.A., and Baarends, W.M. (2009). Dynamic localization of human RAD18 during the cell cycle and a functional

connection with DNA double-strand break repair. DNA Repair (Amst) *8*, 190-201.

Kobayashi, J., Antoccia, A., Tauchi, H., Matsuura, S., and Komatsu, K. (2004). NBS1 and its functional role in the DNA damage response. DNA Repair (Amst) *3*, 855-861.

Masutani, C., Araki, M., Yamada, A., Kusumoto, R., Nogimori, T., Maekawa, T., Iwai, S., and Hanaoka, F. (1999a). Xeroderma pigmentosum variant (XP-V) correcting protein from HeLa cells has a thymine dimer bypass DNA polymerase activity. Embo J *18*, 3491-3501.

Masutani, C., Kusumoto, R., Yamada, A., Dohmae, N., Yokoi, M., Yuasa, M., Araki, M., Iwai, S., Takio, K., and Hanaoka, F. (1999b). The XPV (xeroderma pigmentosum variant) gene encodes human DNA polymerase eta. Nature *399*, 700-704.

Matsuura, S., Kobayashi, J., Tauchi, H., and Komatsu, K. (2004). Nijmegen breakage syndrome and DNA double strand break repair by NBS1 complex. Adv Biophys *38*, 65-80.

Matsuura, S., Tauchi, H., Nakamura, A., Kondo, N., Sakamoto, S., Endo, S., Smeets, D., Solder, B., Belohradsky, B.H., Der Kaloustian, V.M.*, et al.* (1998). Positional cloning of the gene for Nijmegen breakage syndrome. Nat Genet *19*, 179-181.

McCulloch, S.D., Kokoska, R.J., Masutani, C., Iwai, S., Hanaoka, F., and Kunkel, T.A. (2004). Preferential cis-syn thymine dimer bypass by DNA polymerase eta occurs with biased fidelity. Nature *428*, 97-100.

McIlwraith, M.J., Vaisman, A., Liu, Y., Fanning, E., Woodgate, R., and West, S.C. (2005). Human DNA polymerase eta promotes DNA synthesis from strand invasion intermediates of homologous recombination. Mol Cell *20*, 783-792.

Miyase, S., Tateishi, S., Watanabe, K., Tomita, K., Suzuki, K., Inoue, H., and Yamaizumi, M. (2005). Differential regulation of Rad18 through Rad6-dependent mono- and polyubiquitination. J Biol Chem *280*, 515-524.

Mori, T., Nakane, M., Hattori, T., Matsunaga, T., Ihara, M., and Nikaido, O. (1991). Simultaneous establishment of monoclonal antibodies specific for either cyclobutane pyrimidine dimer or (6-4)photoproduct from the same

mouse immunized with ultraviolet-irradiated DNA. Photochem Photobiol *54*, 225-232.

Murai, H., Takeuchi, S., Nakatsu, Y., Ichikawa, M., Yoshino, M., Gondo, Y., Katsuki, M., and Tanaka, K. (2000). Studies of in vivo mutations in rpsL transgene in UVB-irradiated epidermis of XPA-deficient mice. Mutat Res *450*, 181-192.

Nakajima, S., Lan, L., Kanno, S., Usami, N., Kobayashi, K., Mori, M., Shiomi, T., and Yasui, A. (2006). Replication-dependent and -independent responses of RAD18 to DNA damage in human cells. J Biol Chem *281*, 34687-34695.

Nakamura, K., Kato, A., Kobayashi, J., Yanagihara, H., Sakamoto, S., Oliveira, D.V., Shimada, M., Tauchi, H., Suzuki, H., Tashiro, S., *et al.* (2011). Regulation of homologous recombination by RNF20-dependent H2B ubiquitination. Mol Cell *41*, 515-528.

Nishi, R., Alekseev, S., Dinant, C., Hoogstraten, D., Houtsmuller, A.B., Hoeijmakers, J.H., Vermeulen, W., Hanaoka, F., and Sugasawa, K. (2009). UV-DDB-dependent regulation of nucleotide excision repair kinetics in living cells. DNA Repair (Amst) *8*, 767-776.

Oakley, G.G., Tillison, K., Opiyo, S.A., Glanzer, J.G., Horn, J.M., and Patrick, S.M. (2009). Physical interaction between replication protein A (RPA) and MRN: involvement of RPA2 phosphorylation and the N-terminus of RPA1. Biochemistry *48*, 7473-7481.

Ohkumo, T., Kondo, Y., Yokoi, M., Tsukamoto, T., Yamada, A., Sugimoto, T., Kanao, R., Higashi, Y., Kondoh, H., Tatematsu, M., *et al.* (2006). UV-B radiation induces epithelial tumors in mice lacking DNA polymerase eta and mesenchymal tumors in mice deficient for DNA polymerase iota. Mol Cell Biol *26*, 7696-7706.

Richard, G.F., Goellner, G.M., McMurray, C.T., and Haber, J.E. (2000). Recombination-induced CAG trinucleotide repeat expansions in yeast involve the MRE11-RAD50-XRS2 complex. Embo J *19*, 2381-2390.

Stelter, P., and Ulrich, H.D. (2003). Control of spontaneous and damage-induced mutagenesis by SUMO and ubiquitin conjugation. Nature *425*, 188-191.

Szuts, D., Simpson, L.J., Kabani, S., Yamazoe, M., and Sale, J.E. (2006). Role

for RAD18 in homologous recombination in DT40 cells. Mol Cell Biol *26*, 8032-8041.

Tanzanella, C., Antoccia, A., Spadoni, E., di Masi, A., Pecile, V., Demori, E., Varon, R., Marseglia, G.L., Tiepolo, L., and Maraschio, P. (2003). Chromosome instability and nibrin protein variants in NBS heterozygotes. Eur J Hum Genet *11*, 297-303.

Tateishi, S., Niwa, H., Miyazaki, J., Fujimoto, S., Inoue, H., and Yamaizumi, M. (2003). Enhanced genomic instability and defective postreplication repair in RAD18 knockout mouse embryonic stem cells. Mol Cell Biol *23*, 474-481.

Tateishi, S., Sakuraba, Y., Masuyama, S., Inoue, H., and Yamaizumi, M. (2000). Dysfunction of human Rad18 results in defective postreplication repair and hypersensitivity to multiple mutagens. Proc Natl Acad Sci U S A *97*, 7927-7932.

Tauchi, H., Kobayashi, J., Morishima, K., Matsuura, S., Nakamura, A., Shiraishi, T., Ito, E., Masnada, D., Delia, D., and Komatsu, K. (2001). The forkhead-associated domain of NBS1 is essential for nuclear foci formation after irradiation but not essential for hRAD50/hMRE11/NBS1 complex DNA repair activity. J Biol Chem *276*, 12-15.

Tauchi, H., Kobayashi, J., Morishima, K., van Gent, D.C., Shiraishi, T., Verkaik, N.S., vanHeems, D., Ito, E., Nakamura, A., Sonoda, E.*, et al.* (2002). Nbs1 is essential for DNA repair by homologous recombination in higher vertebrate cells. Nature *420*, 93-98.

Terai, K., Abbas, T., Jazaeri, A.A., and Dutta, A. (2010). CRL4(Cdt2) E3 ubiquitin ligase monoubiquitinates PCNA to promote translesion DNA synthesis. Mol Cell *37*, 143-149.

The-International-Nijmegen-Breakage-Syndrome-Study-Group (2000). Nijmegen breakage syndrome. The International Nijmegen Breakage Syndrome Study Group. Arch Dis Child *82*, 400-406.

Ulrich, H.D., and Jentsch, S. (2000). Two RING finger proteins mediate cooperation between ubiquitin-conjugating enzymes in DNA repair. Embo J *19*, 3388-3397.

Uziel, T., Lerenthal, Y., Moyal, L., Andegeko, Y., Mittelman, L., and Shiloh, Y. (2003). Requirement of the MRN complex for ATM activation by DNA

damage. Embo J *22*, 5612-5621.

Varon, R., Dutrannoy, V., Weikert, G., Tanzarella, C., Antoccia, A., Stockl, L., Spadoni, E., Kruger, L.A., di Masi, A., Sperling, K., *et al.* (2006). Mild Nijmegen breakage syndrome phenotype due to alternative splicing. Hum Mol Genet *15*, 679-689.

Varon, R., Vissinga, C., Platzer, M., Cerosaletti, K.M., Chrzanowska, K.H., Saar, K., Beckmann, G., Seemanova, E., Cooper, P.R., Nowak, N.J., *et al.* (1998). Nibrin, a novel DNA double-strand break repair protein, is mutated in Nijmegen breakage syndrome. Cell *93*, 467-476.

Wang, Y., Woodgate, R., McManus, T.P., Mead, S., McCormick, J.J., and Maher, V.M. (2007). Evidence that in xeroderma pigmentosum variant cells, which lack DNA polymerase eta, DNA polymerase iota causes the very high frequency and unique spectrum of UV-induced mutations. Cancer Res *67*, 3018-3026.

Waters, L.S., Minesinger, B.K., Wiltrout, M.E., D'Souza, S., Woodruff, R.V., and Walker, G.C. (2009). Eukaryotic translesion polymerases and their roles and regulation in DNA damage tolerance. Microbiol Mol Biol Rev *73*, 134-154.

Weemaes, C.M., Hustinx, T.W., Scheres, J.M., van Munster, P.J., Bakkeren, J.A., and Taalman, R.D. (1981). A new chromosomal instability disorder: the Nijmegen breakage syndrome. Acta Paediatr Scand *70*, 557-564.

Weemaes, C.M., Smeets, D.F., and van der Burgt, C.J. (1994). Nijmegen Breakage syndrome: a progress report. Int J Radiat Biol *66*, S185-188.

Williams, B.R., Mirzoeva, O.K., Morgan, W.F., Lin, J., Dunnick, W., and Petrini, J.H. (2002). A murine model of Nijmegen breakage syndrome. Curr Biol *12*, 648-653.

Worthylake, D.K., Prakash, S., Prakash, L., and Hill, C.P. (1998). Crystal structure of the Saccharomyces cerevisiae ubiquitin-conjugating enzyme Rad6 at 2.6 A resolution. J Biol Chem *273*, 6271-6276.

Yang, X.H., and Zou, L. (2009). Dual functions of DNA replication forks in checkpoint signaling and PCNA ubiquitination. Cell Cycle *8*, 191-194.

Zhong, H., Bryson, A., Eckersdorff, M., and Ferguson, D.O. (2005). Rad50 depletion impacts upon ATR-dependent DNA damage responses. Hum Mol

Genet *14*, 2685-2693.

Figure legends

Figure 1. NBS1 localization at sites of UV-induced DNA damage and high UV-sensitivity in NBS1-deficient cells. (A) NBS1 localization at UV damage sites was detected in HeLa cells by immunostaining with a CPD antibody 2 hrs after exposure to 100 J/m^2 through a 5 μm filter. White bar indicates 10 μm. (B) Expression of NBS1 species in cells from patients with NBS, 07166VA7 and 0823HSV, NBS1-deficient mouse cells, A31-1 and ΔB/ΔB, and both control HeLa cells and BN$^{+/+}$ cells were determined with Western blot. Immunoprecipitation from the cell extracts was carried out with anti-NBS1 and blotted with NBS1. UV sensitivities of these cell lines were determined with colony formation assay after exposure to 5 J/m^2 UV and the relative sensitivities to that of wild type cells were indicated. Error bars present the standard errors. (C) UV sensitivity of A31-1 cells (closed squares), cells complemented cells NBS1 cDNA (open squares), BN$^{+/+}$ cells (open circles) were determined with colony formation assay after exposure to 5 and 10 J/m^2 UV. Error bars represent the standard errors. Similarly, (D) UV sensitivity of HeLa cells treated with NBS1 siRNA (closed circles), control siRNA (open circles), and HeLa cells treated with NBS1 siRNA

after introduction of the siRNA-resistant NBS1 cDNA (closed triangles) were determined. Error bars represent the standard errors.

Figure 2. The defect in PCNA ubiquitination, recruitment of RAD18 and Pol η in NBS1-deficient cells. (A) Formation of Pol η foci was abolished in A31-1 cells but not in cells complemented with NBS1 full length cDNA and C-terminal (p70:202-754 a.a.) cDNA and in OCN1 cells 4 hrs after exposure to 20 J/m^2. The focus positive cells were defined as more than 10 foci-containing cells. Error bars represent the standard errors. Similarly, (B) PCNA monoubiquitination was suppressed in A31-1 cells, but not in cells complemented with full length cDNA and C-terminus (p70) NBS1 cDNA and BN$^{+/+}$ cells 4 hrs after exposure to 20 J/m^2. (C) Failure of formation of RAD18 foci in A31-1 cells and (D) HeLa cells downregulated with NBS1 siRNA, but not in complemented cells and OCN1 cells 4 hrs after 20 J/m^2 exposure. Error bars indicate the standard errors.

Figure 3. Epistatic analysis between NBS1 and Pol η, and mutation frequency of

NBS1-deficient cells. (A) UV-sensitivities of NBS1- and Pol η -deficient cells were determined by colony forming abilities after UV exposure. 293E cells were down-regulated with NBS1 siRNA and/or Pol η siRNA, and 24 hrs later, cells were irradiated with 2.5, 5, and 10 J/m^2 UV. Error bars represent the standard errors. (B) The mutation frequencies in NBS1- and Pol η -deficient cells were determined by using *rpsL* gene-containing HITEC mouse. HITEC MEF cells were down-regulated with NBS1 siRNA and/or Pol η siRNA, and were irradiated with 5 J/m^2 of UV. After subculturing for 72 hrs, cells were harvested and analyzed for mutation frequencies and the mutation spectrum in *rpsL* gene. Error bars represent the standard errors.

Figure 4. Determination of the RAD18-binding region in NBS1. (A) Time course of interaction of RAD18 and NBS1 in 293E cells after exposure to UV. NBS1 was co-immunoprecipitated with RAD18 antibody in the chromatin fraction after exposure to 20 J/m^2. (B) Illustration of NBS1 deletion mutants at the C-terminus. (C) Failure of interaction of RAD18 with NBS1 clones lacking 639-665 a.a. (D2) and 650-665 a.a. (D2-2) after exposure to 20 J/m^2. Myc-tagged NBS1 and Flag-tagged RAD18 were

prepared according to the method previously described (Miyase et al., 2005; Tauchi et al., 2002). They were co-expressed in human 293E cells and immuunoprecipitated with a Myc antibody in the chromatin fraction 2 hrs after exposure to 20 J/m^2. Asterisks indicate a non-specific band. (D) RAD18 did not localize at the areas of UV damage in A31-1 clones lacking 639-669 a.a. (D2) and 650-665 a.a. (D2-2) 4 hrs after exposure to 100 J/m^2 through 3 μm filter, while other clones showed normal localizations. White bar indicates 10 μm. (E) High UV-sensitivity was detected in NBS1-deficienet cells and a clone lacking 650-665 a.a. (D2-2), but not in the other clones, after exposure to 5 J/m^2. The survivals of each UV-treated A31-1 sample with complemented NBS1 mutants were normalized to the vector-transfected but undamaged A31-1 cells. Error bars represent the standard errors.

Figure 5. RAD6 consensus sequence domain in vertebrate NBS1 at 639-665 a.a. The conserved region of 639-665 a.a. in mammal NBS1 is divided into two sequences 640-643 and 649-663, which correspond to two α-helices, similar to a domain of RAD6. Red letters indicate the consensus a.a. in mammalian NBS1 and their consensus

a.a. in RAD6. N1 and R1 indicate the peptide sequence generated from the RAD6 consensus domain of NBS1 and the corresponding domain of RAD6, respectively.

Figure 6. NBS1-interacting region of RAD18. (A) Illustration of several mutants of RAD18 used in these experiments. (B) Requirement of RAD6-binding domain of RAD18 for interaction with RAD18 and NBS1. Myc-tagged RAD18 and Flag-tagged NBS1 were co-expressed in human 293E cells and immunoprecipitated with a Myc antibody 2 hrs after exposure to 20 J/m^2. (C) Recombinant proteins of RAD18 directly bound to C-terminus of NBS1, but not to N-terminus of NBS1 and to NBS1 D2 mutant lacking 639-669 a.a. (D) Inhibition of interaction between RAD18 and NBS1 in the presence of the N1 peptide in the RAD6-like domain of NBS1 and the R1 peptide in RAD18-binding domain of RAD6, but not peptide C in the ATM-binding domain of NBS1 (see also Figure 5).

Figure 7. NBS1-mediated RAD18 recruitment is facilitated by the homodimer formation through the zinc finger domain.

(A) A single common domain of RAD18 is used for interaction with RAD6 and NBS1. T7-tagged RAD6 and Flag-tagged NBS1 were co-expressed in 293E cells. T7-tagged RAD6 was co-immunoprecipitated with Flag-tagged NBS1 in the presence of RAD18 full length and deletion mutant clones, but not in clones lacking the zinc finger domain, 2 hrs after exposure to 20 J/m^2. (B) Requirement of the zinc finger domain for formation of the RAD18 homodimer. Flag-tagged RAD18 and Myc-tagged RAD18 were co-expressed in 293E cells. Flag-tagged RAD18 was detected by immunoprecipitates with a Myc antibody with full length RAD18 but not in clone lacking the zinc finger 2 hrs after exposure to 20 J/m^2. The RAD6 domain is also required for relocation of RAD18 to chromatin. (C) The time course of RAD18 foci formation in BN$^{+/+}$ cells, A31-1 cells and RAD18$^{-/-}$ cells complemented with RAD18 cDNA (full length and C207F mutant at zinc finger domain). Cells were irradiated with 20 J/m^2 and the RAD18-foci positive cells (more than 10 foci) were counted. Error bars represent the standard errors.

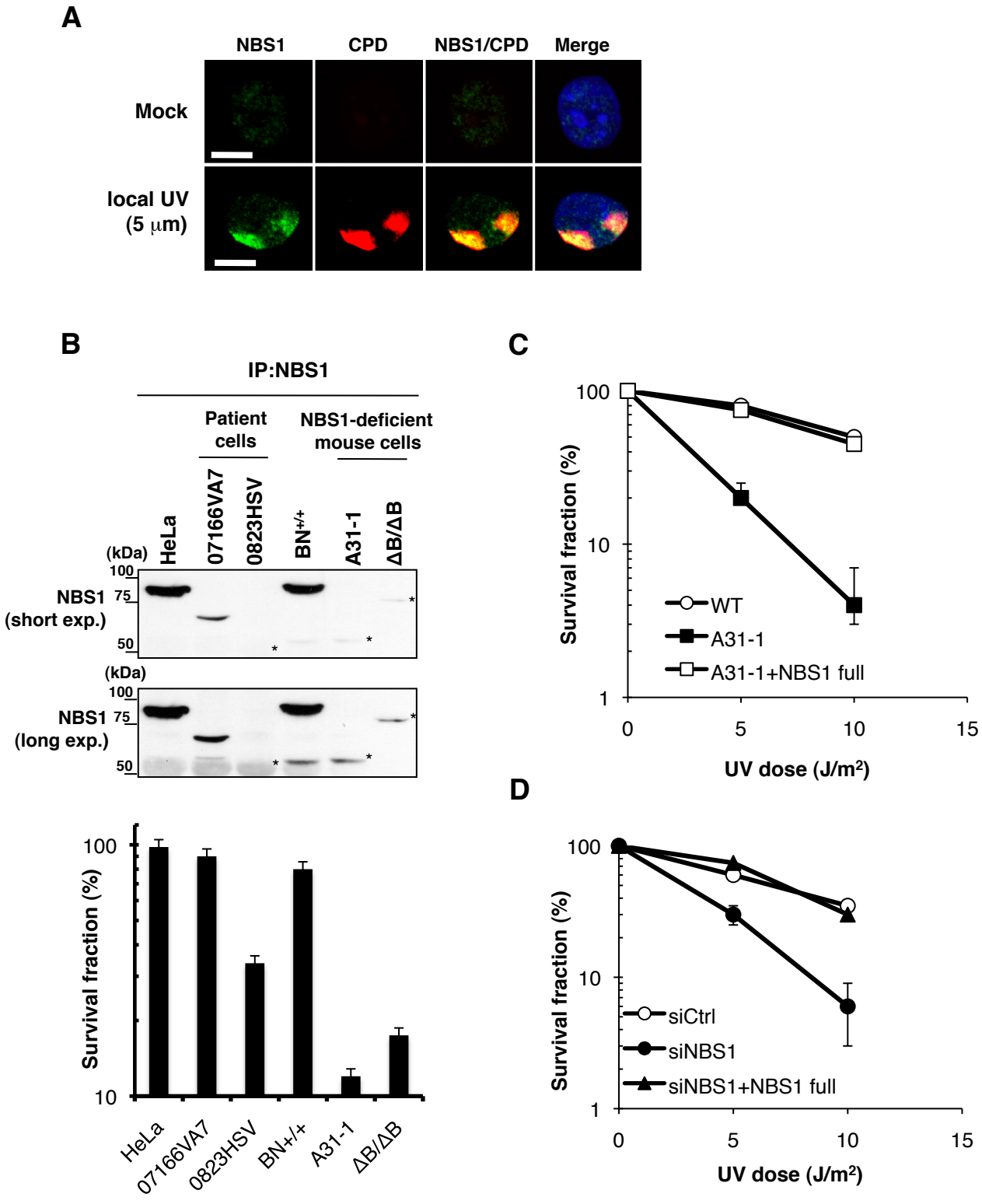

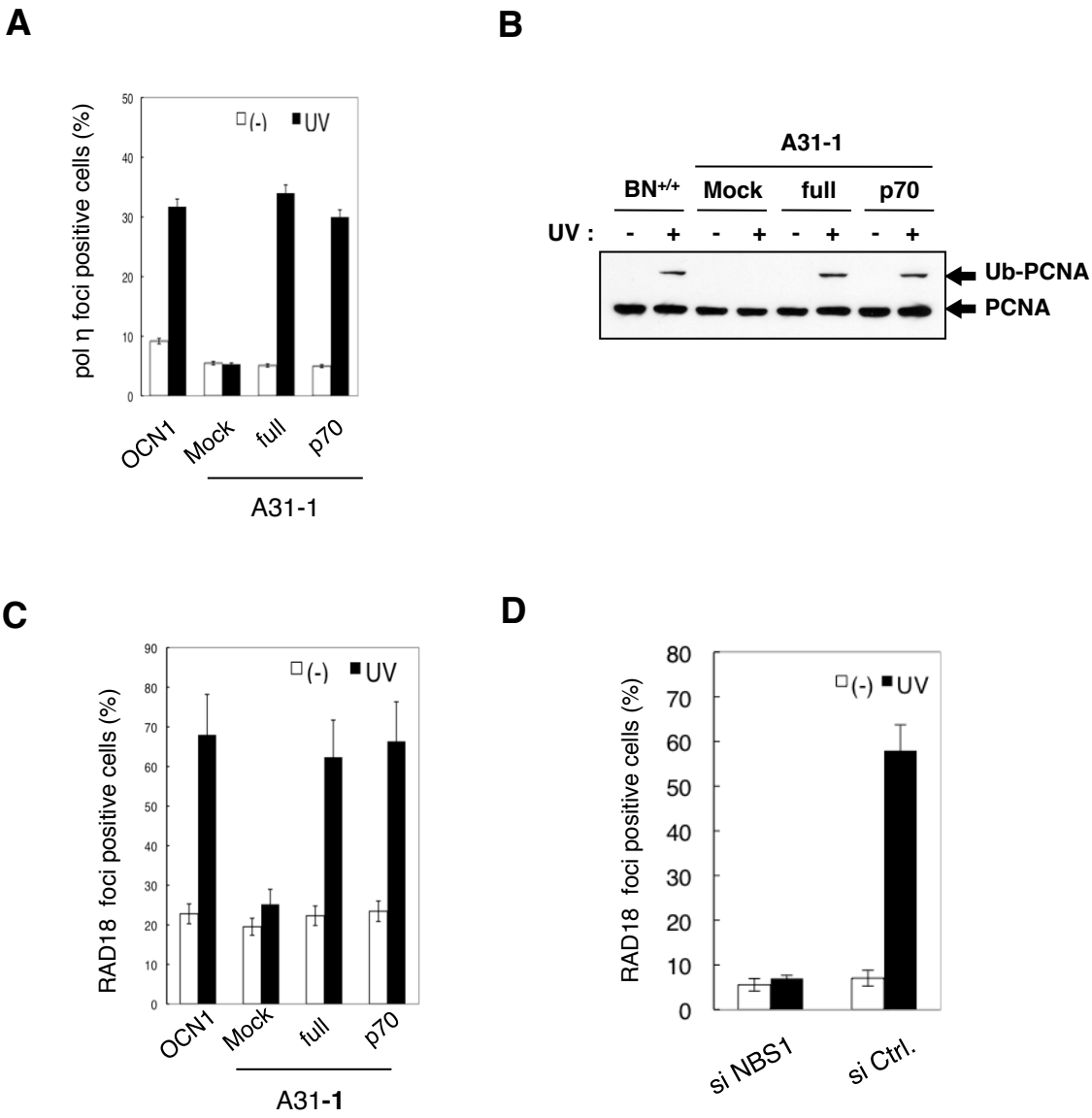

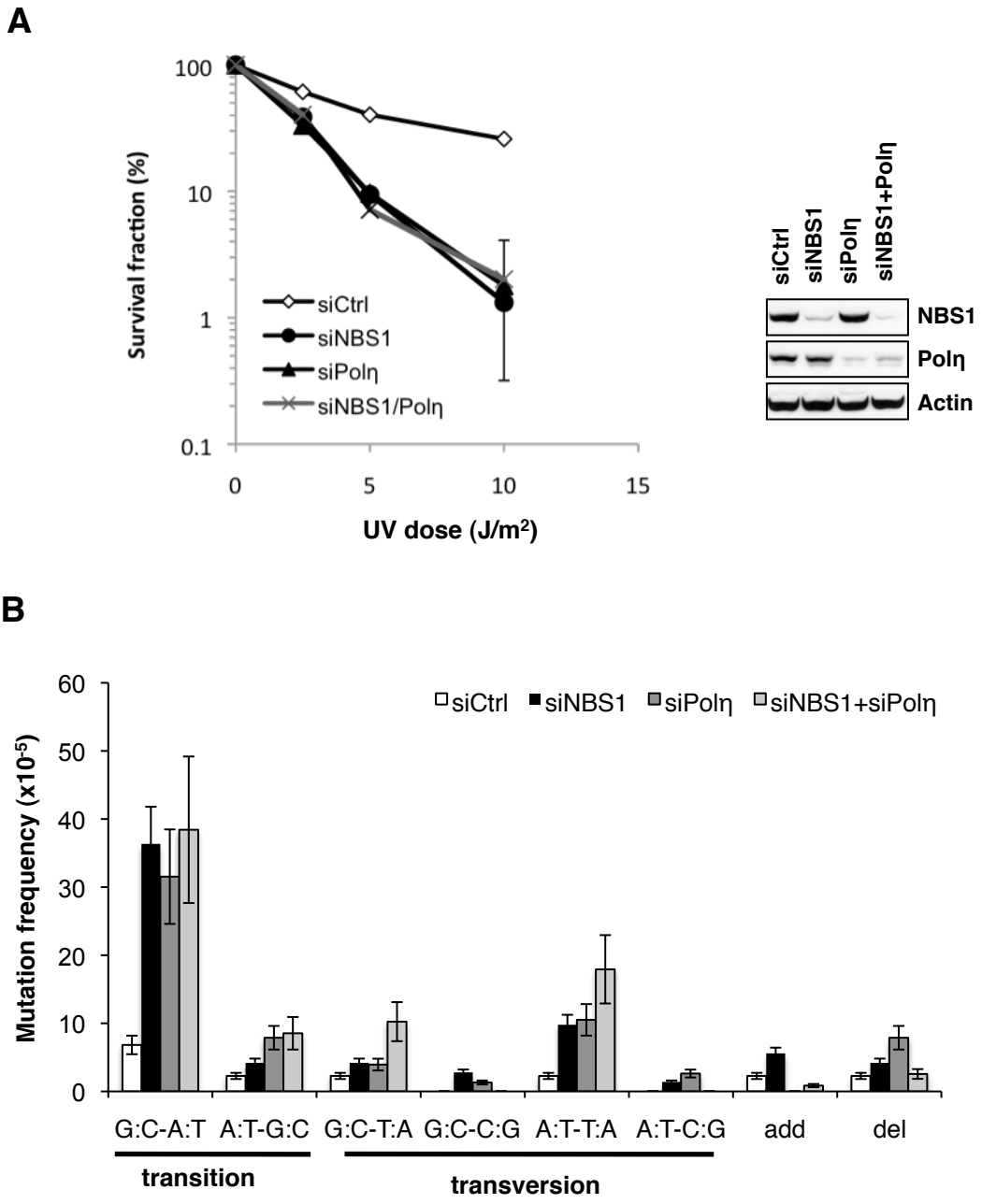

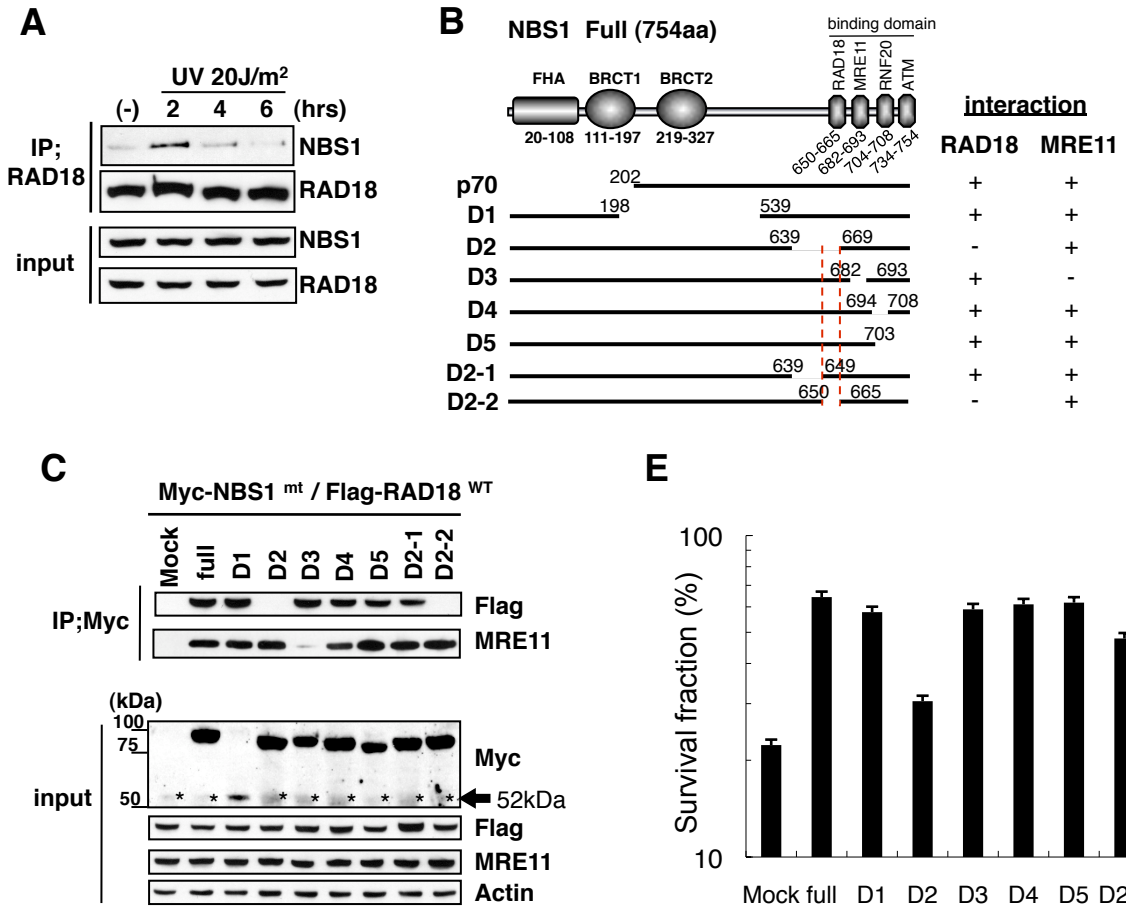

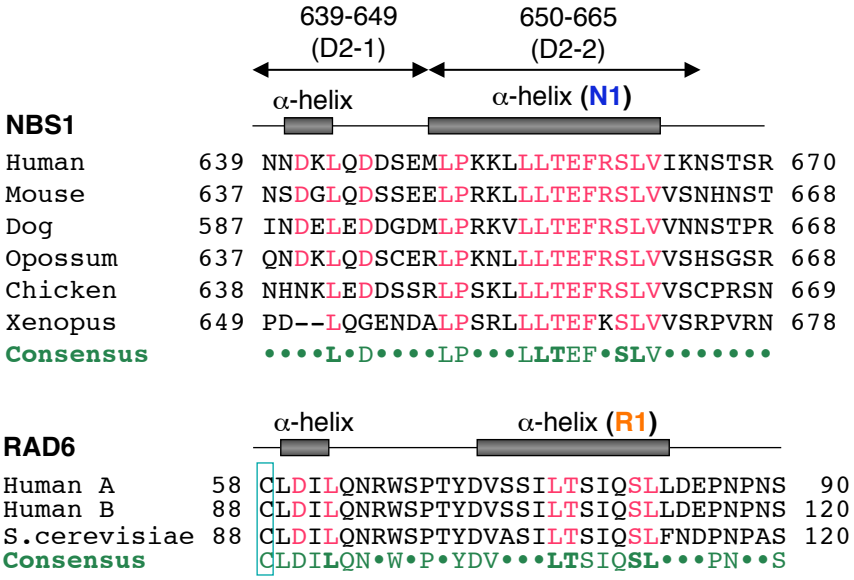

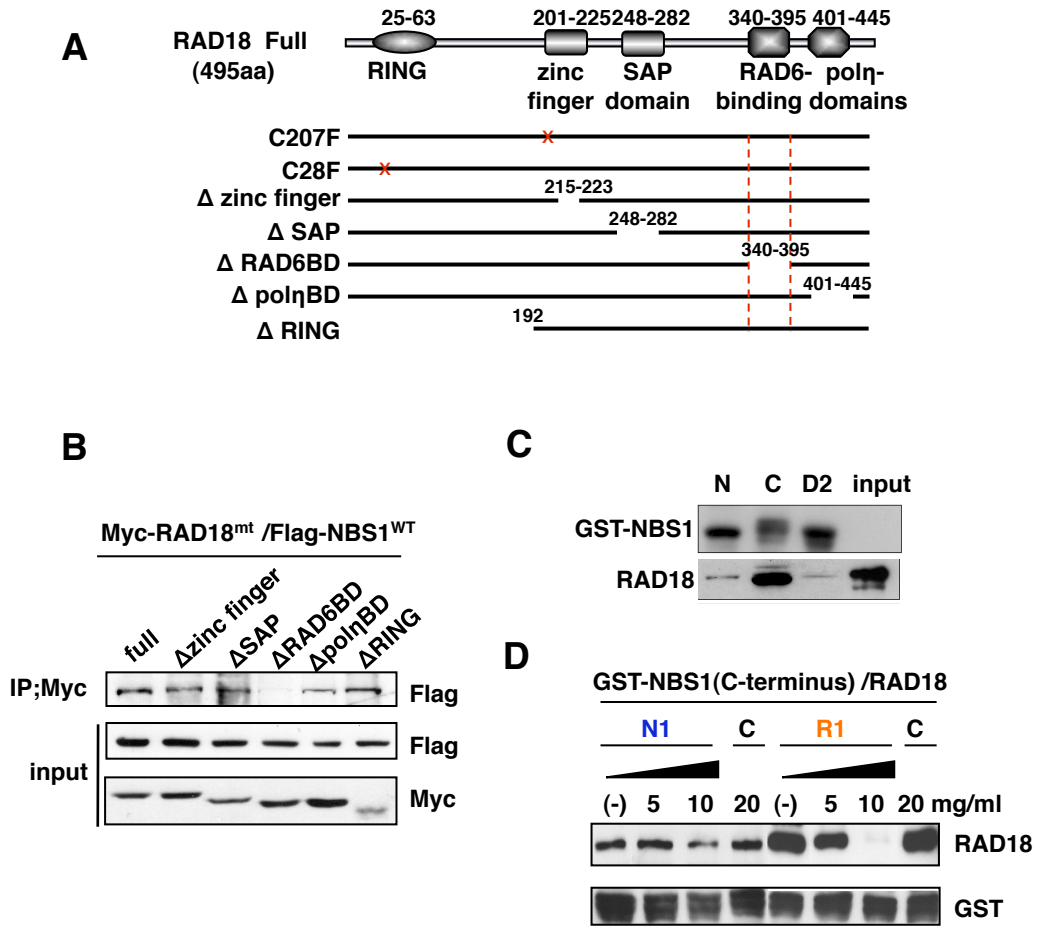

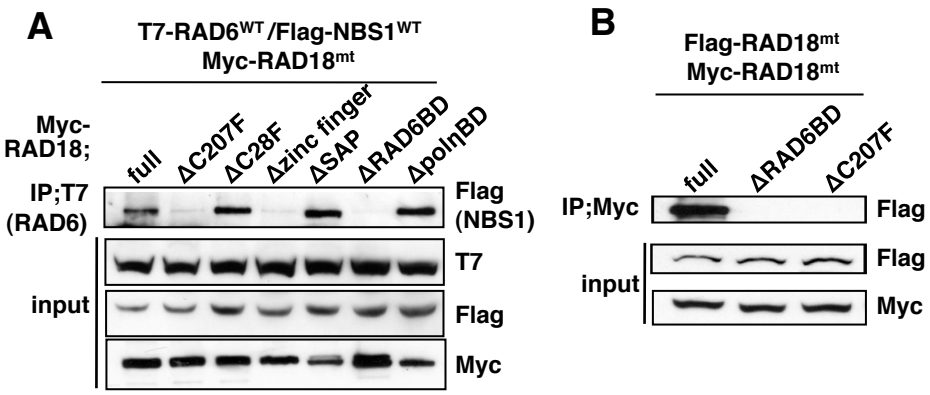

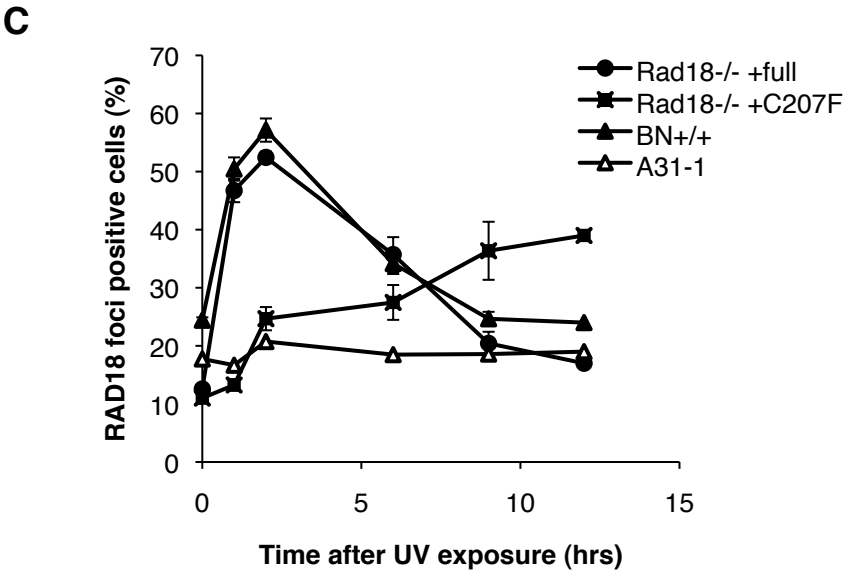

Inventory of Supplemental Information

Information (Supplementary Methods): Laser Microirradiation, UV irradiation and translesion replication, Repair kinetics of UV-induced (6-4) photoproducts and Cell cycle analysis.

References

Figures S1-S7

Supplementary Methods

Laser Microirradiation

U2OS cells were transfected with GFP-NBS1 using FuGENE HD (Roche Applied Science) and cultured for 2 days. Then the cells were treated with Hoechst 33258 (final concentration 4 μg/ml) for 10 minutes and were microirradiated with a 405 nm laser coupled into a Leica TCS SP5 confocal laser scanning microscope.

UV irradiation and translesion replication

Cells were irradiated with 5 J/m^2 of UV and incubated for 30 min. Then pulse-labeled with 10 μCi/mL of [*U*-^{14}C]thymidine (Moravek MC267, 470 mCi/mmol) for 1hr. In a pulse chase experiment, the pulse-labeled cells were incubated further for 5 hrs. These cells were harvested by trypsinization and examined using alkaline sucrose density gradient centrifugation (Takezawa et al., 2008).

Repair kinetics of UV-induced (6-4) photoproducts

Cells were irradiated with 10 J/m^2 of UV and further incubated at 37°C for various times in the presence of 6 mM thymidine to allow for repair of induced photolesions. Genomic DNA was purified from each sample with the QIAamp DNA Blood Mini kit (Qiagen: Hilden, Germany), and the amounts of remaining (6-4) photoproducts were measured by ELISA using the lesion-specific monoclonal antibody as described previously (Katsumi et al., 2001).

Cell cycle analysis

Data acquisition was performed with the CellQuest (Becton, Dickinson and Company) software, and the percentages of G1-, S-, and G2-phase cells were calculated with the MODFIT-LT software program (Verity Software House, Topsham, ME,)

References

Katsumi, S., Kobayashi, N., Imoto, K., Nakagawa, A., Yamashina, Y., Muramatsu, T., Shirai, T., Miyagawa, S., Sugiura, S., Hanaoka, F.*, et al.* (2001). In situ visualization of ultraviolet-light-induced DNA damage repair in locally irradiated human fibroblasts. J Invest Dermatol *117*, 1156-1161.

Takezawa, J., Ishimi, Y., and Yamada, K. (2008). Proteasome inhibitors remarkably prevent translesion replication in cancer cells but not normal cells. Cancer Sci *99*, 863-871.

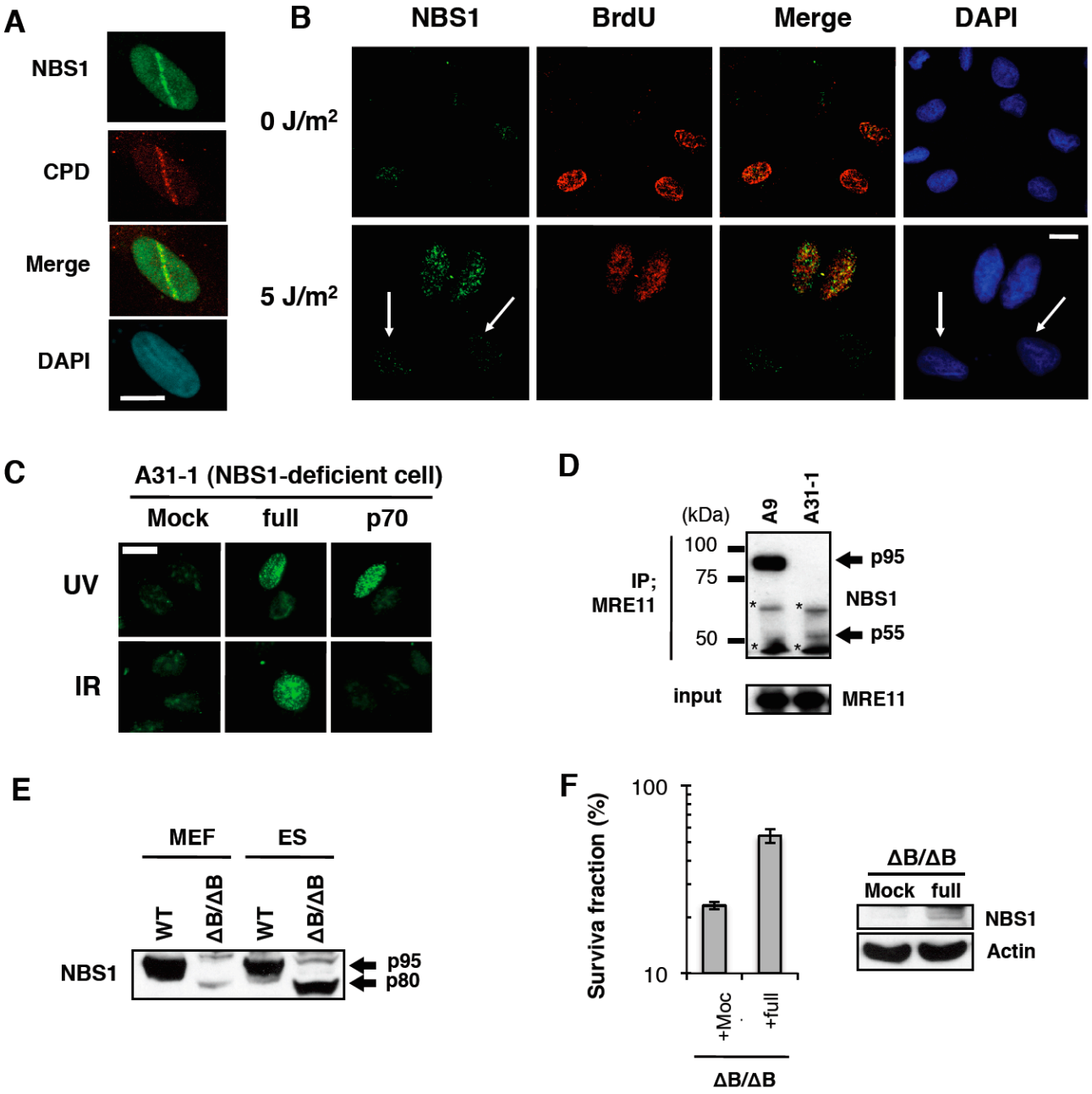

Figure S1. NBS1 localization at sites of UV-lesions through the C-terminus, and the marginal expression of the C-terminus, p55 and p80, in NBS1-deficient mouse cells. (A) NBS1 was recruited to the sites of laser-induced DNA damage. U2OS cells were stained for NBS1 and CPD. (B) NBS1 focus formation is confined to replicating cells, which is stained with BrdU 2 hrs after exposure to 5 J/m^2. White arrow indicates non-proliferating cells. (C) FHA/BRCT domains are dispensable for formation of UV-induced NBS1 focus but not for formation of IR-induced NBS1 focus. A31-1 cells were transfected with NBS1 p70, which lacks FHA/BRCT domains, and submitted to 5Gy (IR) and 20 J/m^2 (UV). After 2 hrs, cells were immunostained with NBS1 antibody, (D) The interaction of MRE11 with the truncated NBS1 (p55) in A31-1 cells. NBS1 in A9 cells or A31-1 cells were co-immunoprecipitated with MRE11 and analyzed by Western blot with NBS1 antibody or MRE11 antibody. Asterisks indicate a non-specific band. (E) The expression level of NBS1 protein in WT cell, ΔB/ΔB ES cells and ΔB/ΔB MEF cells. The cell lysates were analyzed by Western blotting with NBS1 antibody. (F) UV-sensitivity of ΔB/ΔB MEF cells and the restoration by introduction of NBS1 cDNA (full) were determined with colony formation assay after exposure to 5 J/m^2.

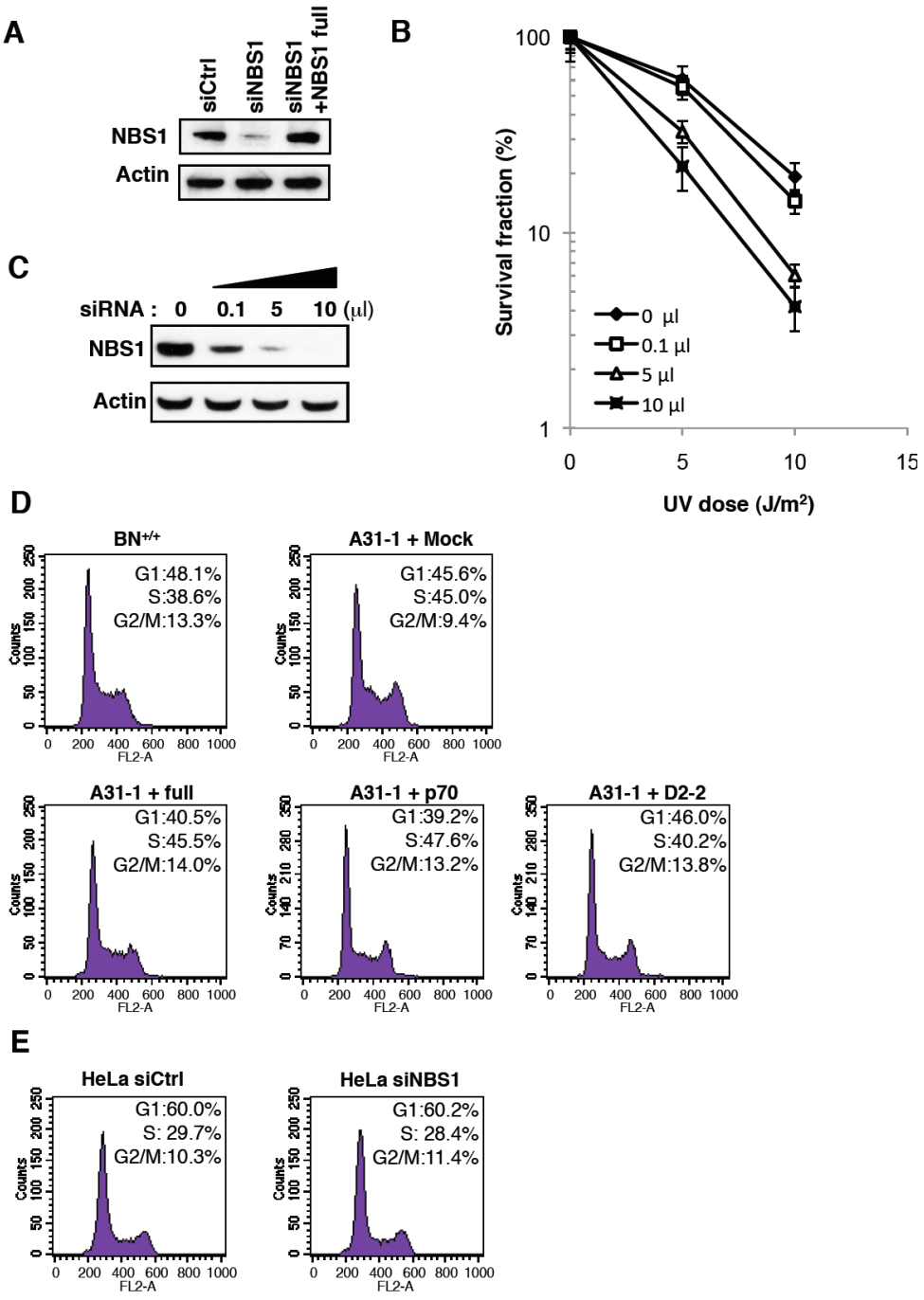

Figure S2. UV-sensitivity associated with the amount of NBS1 expression independently of the cell cycle alteration. (A) NBS1 was significantly reduced by knockdown with 10 µl of siRNA and retrieved by introduction of NBS1 cDNA (full length). (B) The sensitivity of HeLa cells to UV treatment is dependent on the amount of siNBS1 transfected into the cell. (C) NBS1 protein levels in different siRNA concentration. (D) A31-1 cells were transfected with NBS1 (full length), NBS1 (p70) and NBS1 lacking a RAD18-binding domain (D2-2). After 48 hrs, cells were stained with propidium iodide and the distribution of cell-cycle was analyzed with flow cytometry. Similarly, (E) HeLa cells were transfected with control siRNA and NBS1 siRNA, and 48hrs later, the ditribution of cell cycle was determined.

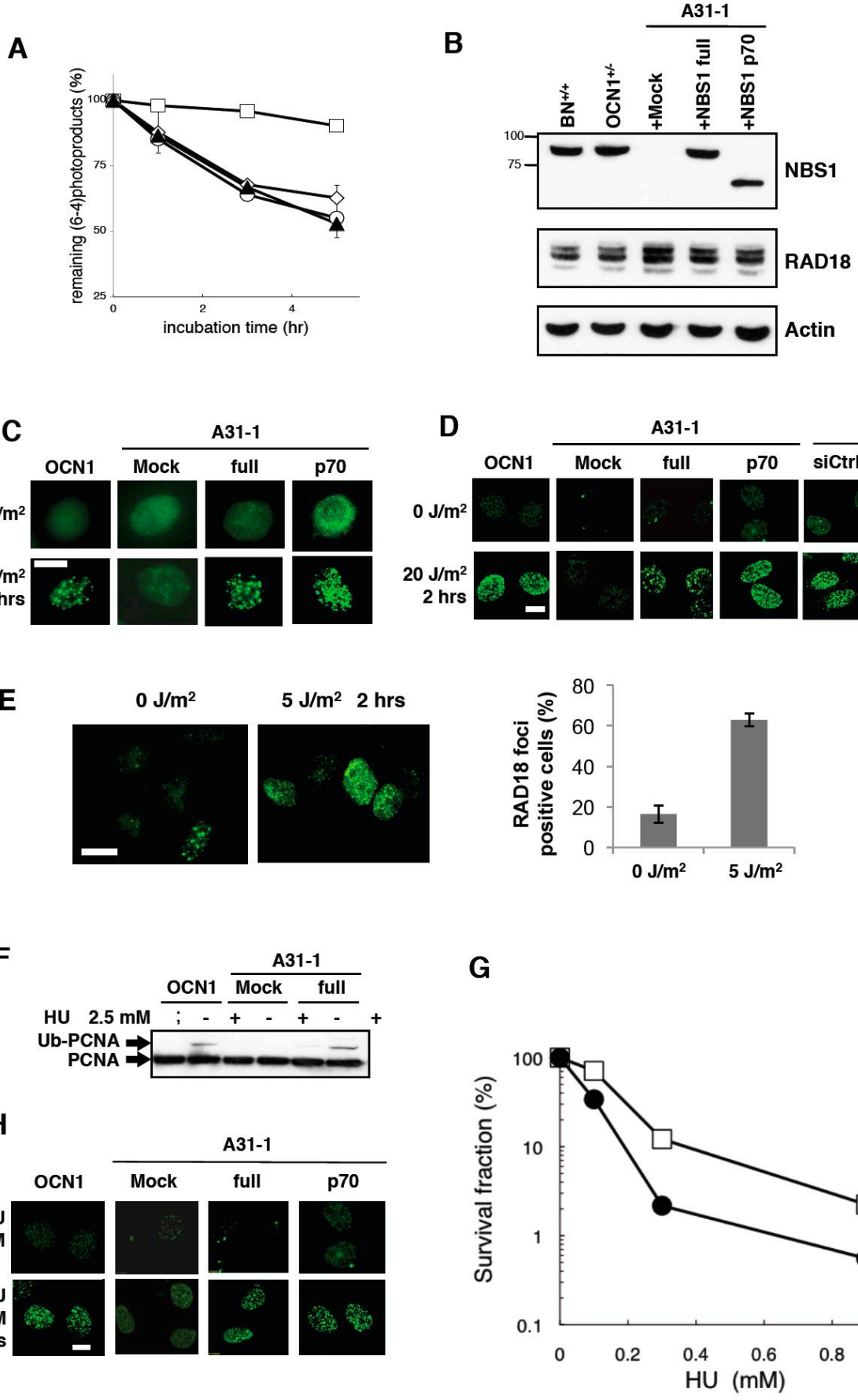

Figure S3. Normal activity of nucleotide excision repair but defect in RAD18 focus formation in NBS1-deficient cells after exposure to UV and HU. (A) Nucleotide excision repair activities in $XPC^{-/-}$ mouse cells (open squares), OCN1 cells (open circles), A31-1 cells (closed triangles) and the cells complemented with NBS1 p70 (open diamonds) were assayed by removal of 6.4 photo-products by ELISA. (B) The expression of NBS1 species were determined in $BN^{+/+}$ cells, OCN1 cells, A31-1 cells and the complemented with NBS1 cDNA (full length or p70). (C) Formation of eGFP-Polη foci was abolished in A31-1 cells, but not in cells complemented with NBS1 cDNA (full length and p70) and OCN1 cells 4 hrs after exposure to 20 J/m^2. White bar indicates 5 μm. (D) RAD18 foci were not formed in A31-1 cells and HeLa cells downregulated with NBS1 siRNA, but formed in cells complemented with NBS1 (full length or p70) and OCN1 cells 2 hrs after 20 J/m^2 exposure. (E) RAD18 foci were increased after exposure to 5 J/m^2 (left panel) and their RAD18 foci-positive cells (containing more than five foci) were quantified (right panel). (F) PCNA mono-ubiquitination in OCN1 cells, A31-1 cells and cells complemented with NBS1 (full length) after treatment with 2.5 mM of HU for 4 hrs. (G) Survival curves in A31-1 cells (closed circles) and cells complemented with NBS1 (full length) (open squares) after treatment with HU for 4 hrs. (H) RAD18 focus formation in OCN1 cells, A31-1 cells and cells complemented with NBS1 (full length or p70) after treatment with 2 mM of HU for 4 hrs. White bar indicates 10 μm.

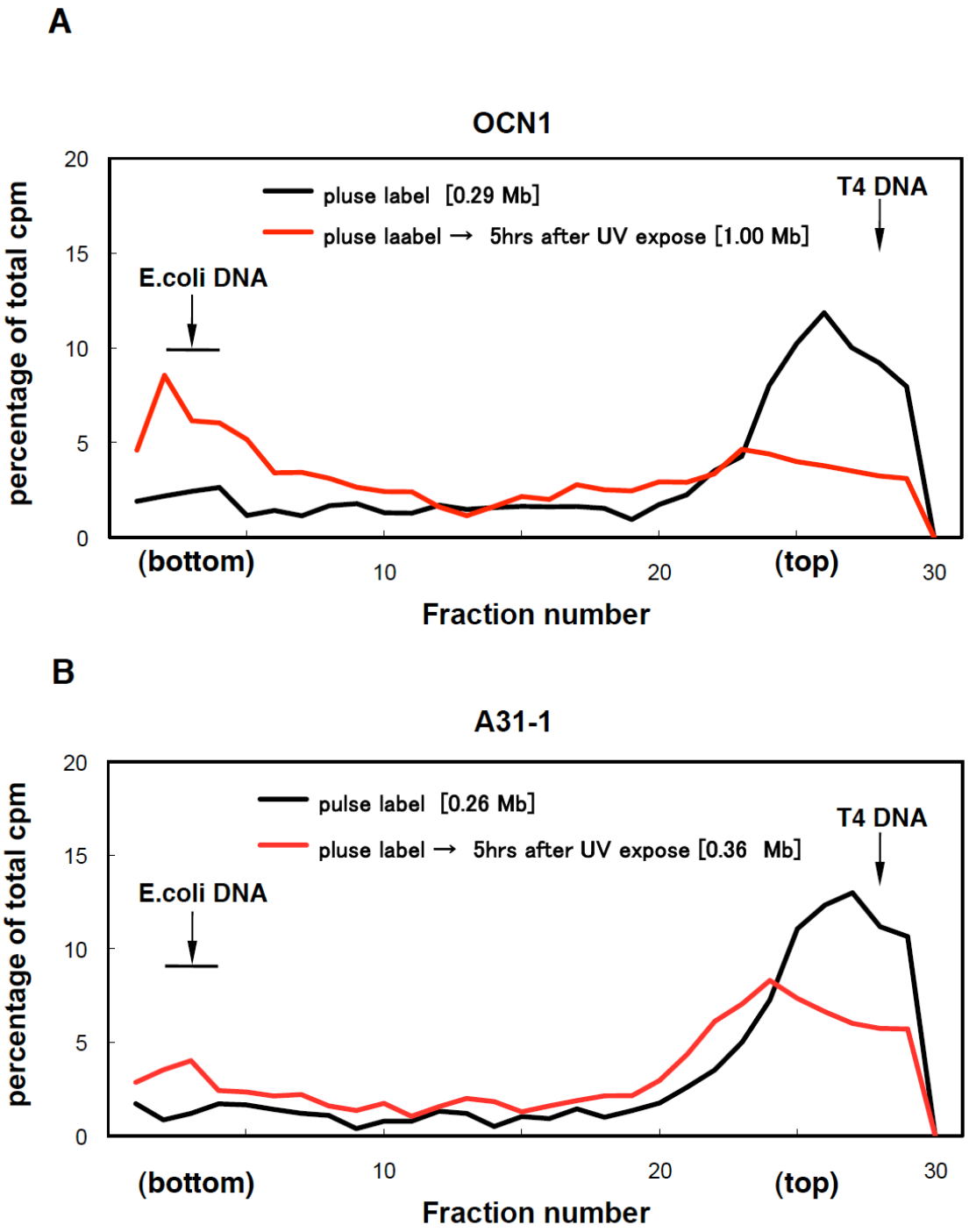

Figure S4. Alkaline sucrose density gradient centrifugation profiles of replication products in NBS1-deficient cells. (A) OCN1 and (B) A31-1 were irradiated with 5 J/m^2, pulse-labeled with 10 μCi/ml of [^{14}C]thymidine for 1hr and incubated for 5 hrs. Sedimentation is from right to left. The arrow indicated the position of the T4 phage DNA (166 kb). Labeled E.coli DNA (approximately 4 Mb) sedimented near the bottom (fraction 3-6). An average fragment length (in megabase) of each profile is shown in square brackets as fragment length of the median fraction, which is the middle fraction that separates the higher half of the profile from the lower half.

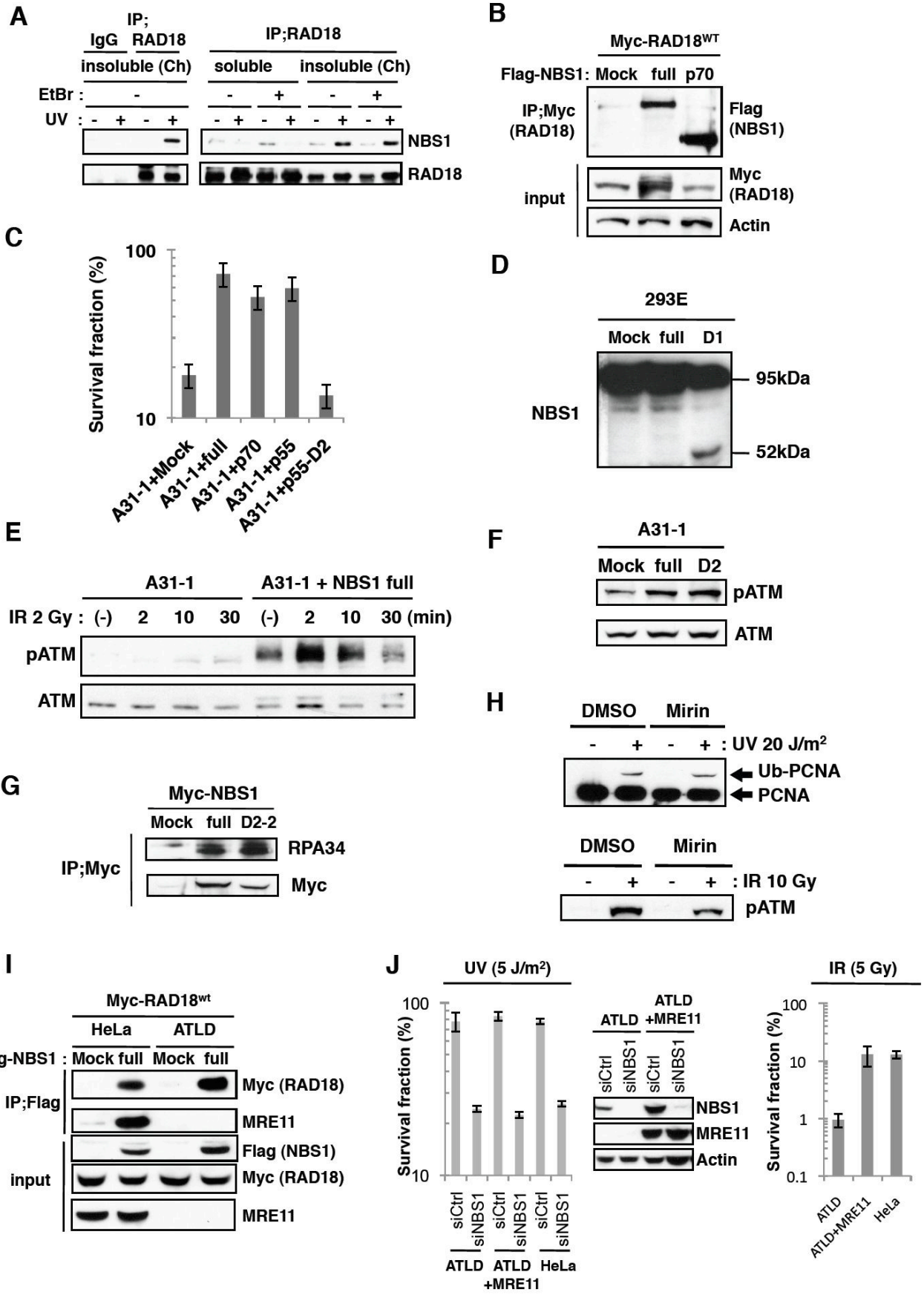

Figure S5. The interaction of NBS1 and RAD18 through the RAD18-binding domain at NBS1 C-terminus, which is not associated with the functions of MRE11 and ATM. (A) The effect of EtBr (50 μg/ml) on the interaction of RAD18 and NBS1 in the chromatin (insoluble) and non-chromatin (soluble) fraction of 293E cells 2 hrs after exposure to 20 J/m^2 of UV. (B) Interaction of RAD18 and NBS1 (full length) or NBS1 p70 in 293E cells 2 hrs after exposure to 20 J/m^2 of UV. (C) UV-sensitivity of A31-1 cells, cells complemented with NBS1 (full length, p70, and p55 with either presence or absence of RAD18-binding domain (D2 mutant), were determined with colony formation assay after exposure to 5 J/m^2. (D) The expression of NBS1 full (95kDa) or D1 (52kDa) in 293E. The cell lysate was analyzed by Western blot with NBS1 antibody. (E) Normal activation of ATM in NBS1 D2 mutant. ATM phosphorylation was reduced in A31-1 cells, (F) but restored in cells complemented with NBS1 (full length) and NBS1 D2 mutant 2 min after exposure to 2 Gy. (G) The interaction of RPA34 with NBS1 (full length) or NBS1 lacking RAD18-binding domain (D2-2 mutant). Myc-tagged NBS1 was co-immuoprecipitated with Myc antibody and analyzed by Western blot with RPA34 antibody. (H) PCNA ubiquitination remained unchanged by a treatment with MRE11 nuclease inhibitor, Mirin, although it significantly affected ATM phosphorylation after IR exposure. HeLa cells were exposed to 20J/m^2 UV in the presence or absence of Mirin (50 μM) and 4 hrs later, PCNA ubiquitination was determined by Western blot with PCNA antibody. Similarly, cells were exposed to 10Gy IR and 30 min later, analyzed by Western blot with pS1981 ATM antibody. (I) Normal interaction of RAD18 and NBS1 in MRE11-deficient ATLD cells. Myc-tagged RAD18 and Flag-tagged NBS1 were co-expressed in ATLD cells and MRE11-proficient HeLa cells, and then Myc-tagged RAD18 was immunoprecipitated with Flag antibody 2 hrs after exposure to 20 J/m^2. (J) UV-sensitivity of ATLD cells, ATLD cells complemented with MRE11, HeLa cells and their counterparts transfected with NBS1 siRNA. UV-sensitivity of ATLD cells was similar to that of cells complemented with MRE11 and HeLa cells, although it was significantly enhanced by depletion of NBS1 (left panel). ATLD cells were sensitive to IR with 5 Gy and, after complementation with MRE11, they were restored to normal sensitivity at the level of HeLa cells (right panel).

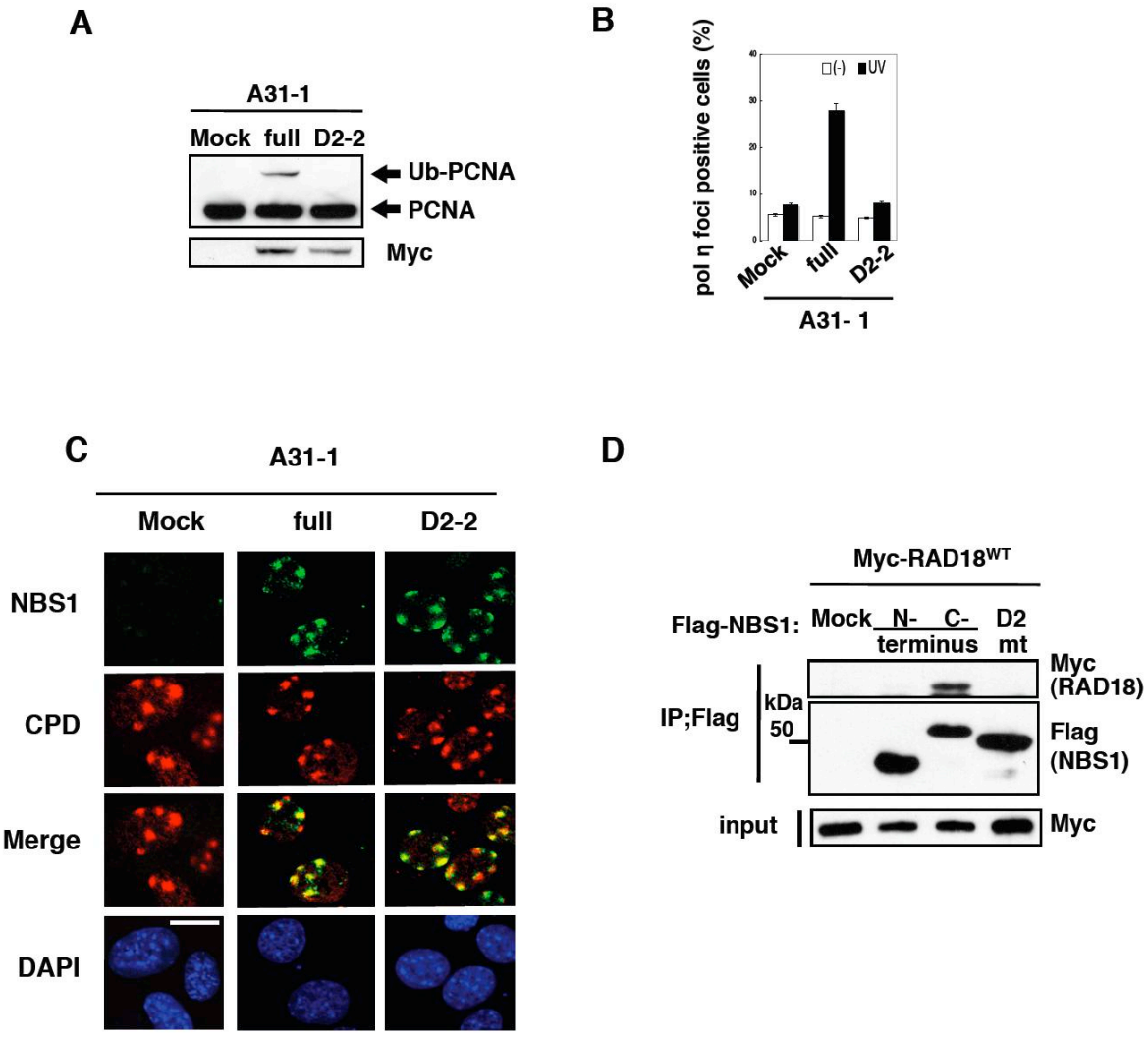

Figure S6. The requirement of RAD18 binding domain for both PCNA ubiquitination and Polη focus formation, but not for recruitment of NBS1 to sites of UV-lesions. A31-1 cells lacking 650-665 a.a. (D2-2) were failed to restore PCNA ubiquitination 4 hrs after exposure to 20 J/m^2 (A) and Polη focus formation (B). Error bars indicate the standard errors. (C) UV-induced NBS1 foci were robustly formed in A31-1 clone lacking the 650-665 a.a. (D2-2) 4 hrs after exposure to 100 J/m^2 through 3 μm filter. (D) NBS1 interacts with RAD18 through RAD18 binding domain at NBS1 C-terminus after exposure to 5 J/m^2. Flag-tagged NBS1 N-terminus, NBS1 C-terminus in either presence or absence of RAD18-binding domain (D2 mutant) were introduced to 293E cells, which contained Myc-tagged RAD18, and then, the immuno-precipitates with Flag antibody were analyzed by Western blot with Myc or Flag antibody.

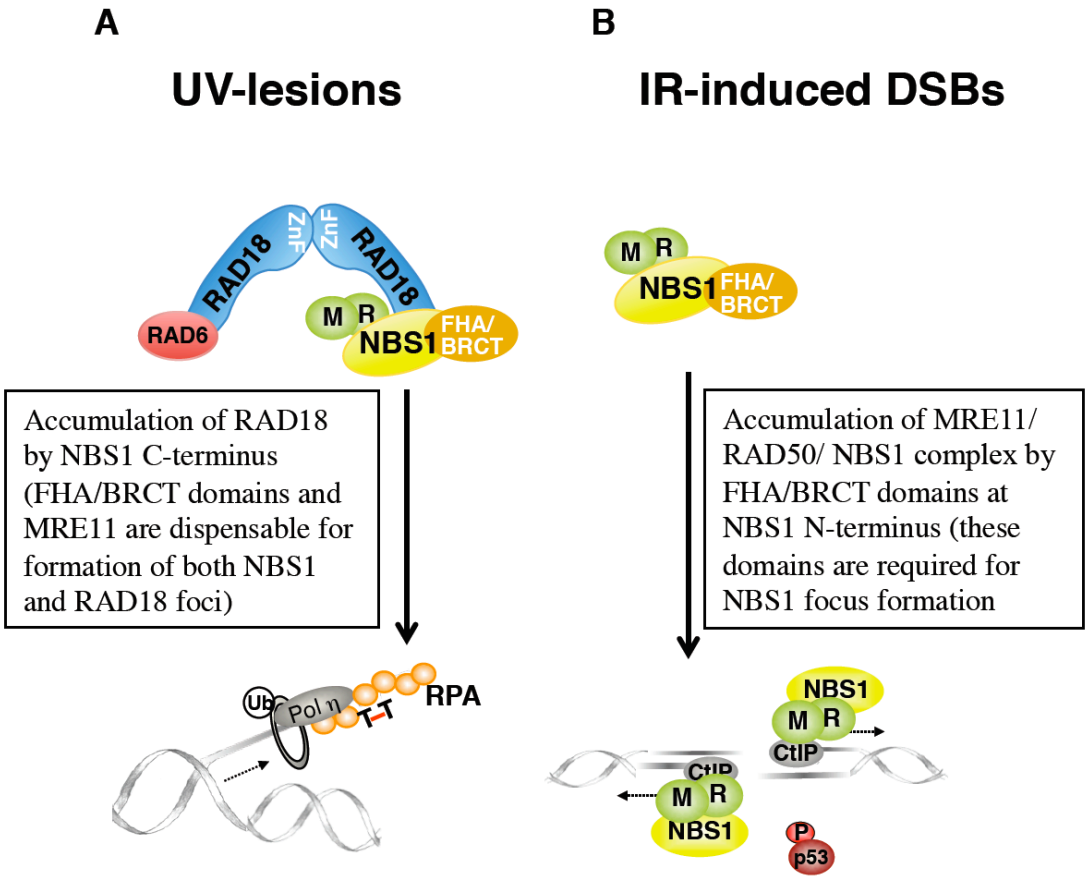

Figure S7. Model for interaction of RAD18 with NBS1. (A) RAD18 homodimers simultaneously interact with NBS1 and RAD6, and accumulate at sites of UV-lesions by NBS1 C-terminus. (B) MRE11/RAD50 (MR) / NBS1 complex accumulates at sites of IR-induced DSBs by FHA/BRCT domains at NBS1 N-terminus.